HHS Public Access

Author manuscript

Toxicology. Author manuscript; available in PMC 2024 May 16.

Published in final edited form as:

Toxicology. 2023 December ; 500: 153692. doi:10.1016/j.tox.2023.153692.

Lack of Mitochondrial Cyp2E1 Drives Acetaminophen-induced ER Stress-mediated Apoptosis in Mouse and Human Kidneys: Inhibition by 4-Methylpyrazole but not N-Acetylcysteine

Jephte Y. Akakpo[1], **Anup Ramachandran**[1], **Barry H. Rumack**[2], **Darren P. Wallace**[3], **Hartmut Jaeschke**[1]

[1]Department of Pharmacology, Toxicology & Therapeutics, University of Kansas Medical Center, Kansas City, KS, USA.

[2]Department of Emergency Medicine and Pediatrics, University of Colorado School of Medicine, Denver, CO, USA.

[3]Jared Grantham Kidney Institute, University of Kansas Medical Center, Kansas City, KS, USA.

Abstract

Acetaminophen (APAP) overdose causes liver injury and acute liver failure, as well as acute kidney injury, which is not prevented by the clinical antidote N-acetyl-L-cysteine (NAC). The absence of therapeutics targeting APAP-induced nephrotoxicity is due to gaps in understanding the mechanisms of renal injury. APAP metabolism through Cyp2E1 drives cell death in both the liver and kidney. We demonstrate that Cyp2E1 is localized to the proximal tubular cells in mouse and human kidneys. Virtually all the Cyp2E1 in kidney cells is in the endoplasmic reticulum (ER), not in mitochondria. By contrast, hepatic Cyp2E1 is in both the ER and mitochondria of hepatocytes. Consistent with this subcellular localization, a dose of 600 mg/kg APAP in fasted C57BL/6J mice induced the formation of APAP protein adducts predominantly in mitochondria of hepatocytes, but the ER of the proximal tubular cells of the kidney. We found that reactive metabolite formation triggered ER stress-mediated activation of caspase-12 and apoptotic cell death in the kidney. While co-treatment with 4-methylpyrazole (4MP; fomepizole) or the caspase inhibitor Ac-DEVD-CHO prevented APAP-induced cleavage of procaspase-12 and apoptosis in the kidney, treatment with NAC had no effect. These mechanisms are clinically relevant because 4MP but not NAC also significantly attenuated APAP-induced apoptotic cell death in primary human kidney cells. We conclude that reactive metabolite formation by Cyp2E1 in the ER results in sustained ER stress that causes activation of procaspase-12, triggering apoptosis of proximal tubular cells, and that 4MP but not NAC may be an effective antidote against APAP-induced kidney injury.

Keywords

acetaminophen nephrotoxicity; acetaminophen hepatotoxicity; ER stress; apoptosis; fomepizole; Cyp2E1

For Correspondence: Hartmut Jaeschke, PhD., University of Kansas Medical Center, Department of Pharmacology, Toxicology & Therapeutics, 3901 Rainbow Blvd, MS 1018, Kansas City, KS, 66160, USA. hjaeschke@kumc.edu.

INTRODUCTION

Acetaminophen (APAP) is a safe analgesic and antipyretic drug commonly used as a pain reliever and fever reducer. However, an APAP overdose is often associated with hepatotoxicity and is the major cause of acute liver failure (ALF) in the U.S. (Fisher and Curry, 2019; Hodgman and Garrard, 2012; Jaeschke, 2015). Though the liver is the main target organ for toxic APAP ingestions, a high overdose can also cause renal dysfunction and acute kidney injury (AKI) (Akakpo et al., 2020; Hengy et al., 2009; McClain et al., 1988). Although AKI is common in ALF patients and affects both short- and long-term outcomes, it generally does not cause chronic kidney disease (Tujios et al., 2015). Interestingly, there is also evidence indicating that renal failure can develop in APAP overdose patients without liver failure suggesting a direct effect of APAP on the kidney (Campbell and Baylis, 1992; Eguia and Materson, 1997). Moreover, the only available treatment for an APAP overdose is N-acetyl-L-cysteine (NAC), which does not protect against APAP-induced nephrotoxicity in mice (Slitt et al., 2004) and no benefit has been reported in patients (Mazer and Perrone, 2008; Mour et al., 2005). Thus, there are no clinical interventions that can prevent or improve APAP-induced AKI. The main reason for this is the lack of a clear understanding of the mechanisms of APAP nephrotoxicity.

Drug metabolism by cytochrome P450 2E1 (Cyp2E1) is an important step in APAP-induced injury to renal proximal tubules leading to the formation of the reactive metabolite, N-acetyl-p-benzoquinone imine (NAPQI) (Akakpo et al., 2020; Hart et al., 1995; Hu et al., 1990). This metabolic activation of APAP leads to extensive GSH depletion and then covalent binding of NAPQI to proteins, which initiates nephrotoxicity (Akakpo et al., 2020; Hart et al., 1994). APAP-induced cell death in the liver is almost exclusively necrosis (Gujral et al., 2002); however, in isolated tubular epithelial cells, cell death may also involve apoptosis (Lorz et al., 2005). The detailed mechanistic steps between the Cyp2E1-mediated formation of NAPQI protein adducts and the induction of cell death in the kidney *in vivo* need to be clarified.

Mitochondrial dysfunction has been suggested to play a central role in APAP-induced apoptotic renal cell death (Shen et al., 2020; Wei et al., 2023). However, further examination of the molecular signaling of APAP nephrotoxicity also found that the mitochondrial pathway was not activated during APAP-induced cell death, and no dissipation of mitochondrial membrane potential, mitochondrial Bax translocation, or release of cytochrome C was detected *in vitro* (Lorz et al., 2005). Consistently, we found that while APAP protein adducts are formed in the whole kidney tissue homogenates, mitochondrial adducts are not produced (Akakpo et al., 2020). Notably, APAP can promote ER stress-mediated apoptosis in primary cultures of murine proximal tubular epithelial cells through caspase-12 without mitochondrial dysfunction (Lorz et al., 2004). Moreover, the activity of Cyp2E1 has recently been demonstrated to be predominantly localized to the ER of human kidneys (Arzuk et al., 2022). Thus, a mechanistically distinct mode of ER stress-mediated renal apoptotic cell death during APAP nephrotoxicity may be more relevant to the mouse and human pathology.

Apoptosis is a compensatory form of programmed cell death that is mediated by several signaling pathways, which can be activated by proapoptotic agents (Ortiz et al., 2003). We have previously demonstrated that significant oxidative metabolism of APAP occurs in the kidneys which is prevented via Cyp2E1 inhibition by 4-methylpyrazole (4MP, fomepizole) (Akakpo et al., 2020). 4MP is an FDA-approved antidote against methanol and ethylene glycol poisoning in humans because it is a potent inhibitor of alcohol dehydrogenase (McMartin, 2010). 4MP is now being evaluated as a new therapeutic option in a phase III clinical trial to manage acute liver injury in patients after APAP overdose (Akakpo et al., 2022b). However, the effect of 4MP against APAP-induced ER stress and apoptotic signaling in the kidney *in vivo* has not been investigated. Hence, our study was designed to compare the protective effect of 4MP and NAC, which is the standard of care, on APAP-induced renal apoptosis in the human-relevant mouse model and in primary human kidney cells. In addition, we assessed why there is a fundamentally different mechanism of cell death in the kidney compared to the liver, despite the same metabolic activation of APAP by Cyp2E1.

MATERIALS AND METHODS

Animals and experimental design

All animal experiments were approved by the Institutional Animal Care and Use Committee (IACUC) at the University of Kansas Medical Center (Protocol number: 21-12-212; approved on 1/18/2022) and conducted in accordance with the National Institute of Health and the National Research Council for the care and use of laboratory animals' guidelines. Eight to ten-week-old male C57BL/6J mice (average body weight of 20-25 g) were purchased from Jackson Laboratories (Jackson Lab, Harbor, Maine) and acclimated for 5 days. Before experiments, animals were fasted overnight and then treated intraperitoneally with 10 ml/kg saline alone or 600 mg/kg APAP (Sigma-Aldrich, St. Louis, MO) dissolved in warm saline. The high overdose of APAP is necessary to induce not only the liver but also acute kidney injury consistent with the observation in patients (Akakpo et al., 2020). Some mice were pretreated with 3 mg/kg Ac-DEVD-CHO (Bajt et al., 2001; Boyle et al., 2013) 30 min before APAP treatment. Additional groups of mice received a cotreatment of APAP with 50 mg/kg 4MP (Sigma-Aldrich) (Akakpo et al., 2020) or 500 mg/kg NAC (Akakpo et al., 2019). Animals were euthanized under isoflurane anesthesia at 6 or 24 h post-APAP followed by collection of blood, kidney, and liver samples. All chemicals were dissolved in warm saline.

Biochemical measurements

Heparinized mouse blood samples were centrifuged at 20,000×g for 3 min at 4°C to collect plasma. To assess the extent of kidney injury, blood urea nitrogen (BUN) was measured using a QuantiChrom™ Urea Assay kit from BioAssay Systems (Hayward, CA). To assess the extent of liver injury, alanine aminotransferase (ALT) activity was measured with a kit purchased from Point Scientific Inc (Canton, MI). Cell death in cultured cells was assessed by lactate dehydrogenase (LDH) release, as described in detail (Bajt et al., 2004).

Histology

After kidney and liver tissue collections, samples were fixed in 10% formalin for 16 hours. Fixed tissue samples were then embedded in paraffin and 5 μm sections were cut. To evaluate the extent of tubular and glomerular damage in the kidney and assess the extent of necrotic cell death in the liver, sections were stained with hematoxylin & eosin (H&E). DNA fragmentation was assessed in tissue sections by the terminal deoxynucleotidyl transferase-mediated dUTP nick end-labeling (TUNEL) assay with the in-situ Death Detection Kit, AP (Roche Diagnostics, Indianapolis, IN).

Primary human kidney cell isolation and treatments

Normal human kidney (NHK) cells were isolated by the PKD Biomarkers and Biomaterials Core at KUMC as described in detail (Wallace and Reif, 2019). Kidney tissues were obtained from nephrectomy specimens by the surgery department or from the Midwest Transplant Network (Kansas City, MO). The use of de-identified surgically discarded tissues complies with federal regulations and was approved by the Institutional Review Board (IRB) at KUMC. NHK were seeded on collagen-coated plates in DMEM/F12 + P/S + ITS + 10% FBS and allowed to attach and proliferate in a humidified 5% CO_2 incubator (at 37°C) for 2 days. The adherent NHK cells were washed with sterile phosphate-buffered saline (PBS) and a starvation media consisting of DMEM/F12 + P/S + ITS + 0.5% FBS was added for 3 hours. NHK cells were either treated with 1, 5, or 10 mM APAP with or without 2 mM 4MP, 20 mM NAC (Akakpo et al., 2021), 20 μM Ac-DEVD-CHO for 24 or 48 h (Gyrd-Hansen et al., 2006) or 100, 200, and 300 μM TUDCA. All drugs were dissolved in saline.

Immunostaining

Immunostaining of mouse and human kidney samples was performed on paraffin-embedded tissue sections cut at 5 μm thickness. Briefly, tissues were first deparaffinized, dehydrated, and then blocked with 5% normal goat serum. Then, overnight incubation was performed with the following primary antibodies: anti-Cyp2E1 (Cat. # ab28146, Abcam, Boston, MA), anti-SGLT2 (Cat. # 20802, Bicell Scientific St. Louis, MO), Santa Cruz, Dallas, TX). The next day, sections were washed in PBS before application of the secondary antibodies, Alexa Fluor 594-conjugated goat anti-rabbit antibody and Alexa Fluor 488-conjugated goat anti-mouse antibody (Cat. # A11037 & A-11001), ThermoFisher Scientific, Waltham, MA). Once nuclei were stained with a DAPI-containing mounting medium (Life Technologies), slides were imaged on an inverted fluorescence microscope. NHK cells were fixed using 4% formalin for 10 min before washing with cold PBS 3 times. The cells were then blocked in 1% BSA in PBS for 30 min at room temperature before incubation with anti-Cyp2E1 (Cat. # ab28146, Abcam) and anti-SGLT-2 (Cat. # (Cat. # 20802, Bicell Scientific) antibodies at 4°C overnight. The next day, goat anti-mouse secondary antibody linked to Alexa Fluor 488- and Alexa Fluor 594-conjugated goat anti-rabbit antibodies were added for 60 min at room temperature, followed by imaging on a Nikon Eclipse Ti2 Inverted microscope.

Western blotting

Tissue samples were homogenized in ice cold isolation buffer (pH 7.4) containing 220 mM mannitol, 70 mM sucrose, 2.5 mM HEPES, 10 mM EDTA, 1 mM EGTA, and 0.1%

bovine serum albumin. This was followed by total protein measurements with the BCA assay from Pierce Scientific (Waltham, Ma). Western blotting was then carried out with the following antibodies to cytochrome P450 2E1 (Abcam rabbit polyclonal antibody, Cat. # ab28146), NGAL (Santa Cruz, Cat. # Sc-515876), ß-actin (Cell Signaling, Cat. # 4967), PDI (Santa Cruz, Cat. #Sc-74551), GRP78 (Santa Cruz, Cat. # Sc-166490), CHOP (Santa Cruz, Cat. # Sc-166682), pro caspase-12 and cleaved caspase-12 (Cell Signaling, Cat. #35965), porin (Abcam, cat. #ab14734), and calreticulin (Cell Signaling, Cat. #12238). Anti-rabbit or anti-mouse IgG horseradish peroxidase coupled secondary antibodies (Santa Cruz Biotechnology) (1:5000 dilution), coupled with the ECL kit from Amersham (Piscataway, NJ) were then used for detection of protein bands by chemiluminescence on the LI-COR Odyssey imaging system (LI-COR Biosciences).

Subcellular fractionation and isolation of mitochondria and ER

Mitochondria and ER were isolated from mouse and human tissue homogenates by ultracentrifugation. Briefly, freshly collected liver and kidney tissue samples were minced and homogenized in ice-cold isolation buffer (pH 7.4, containing 22 mM mannitol, 70 mM sucrose, 2.5 mM 4-(2-hydroxyethyl)-1-piperazineethanesulfonic acid (HEPES), 10 mM EDTA, 1 mM ethylene glycol tetra acetic acid, and 0.1% bovine serum albumin). Cell debris was removed by spinning the homogenate at 2,500 g for 10 min. The resultant supernatant was centrifuged at 20,000 × g for 10 min to pellet mitochondria which was then subjected to 3 rounds of a washing step in the ice-cold buffer. After centrifugation, the supernatant was ultracentrifuged at 100,000 × g for 1 h, to pellet the ER, which was also subjected to 3 additional washes in the ice-cold buffer at 100,000 × g for 60 min. Both mitochondrial and microsomal fractions were flash-frozen and stored at −80°C.

Quantitation of APAP protein adducts

Measurements of APAP-CYS derived from APAP protein adducts were performed as previously described (Akakpo et al., 2020; McGill et al., 2013). Briefly, mitochondrial and microsomal fractions of the kidney and liver were filtered through a Bio-Spin 6 column from Bio-Rad (Hercules, CA) to remove low molecular weight metabolites that could interfere with the detection of APAP protein adducts (McGill et al., 2013). Isolated APAP-CYS residues were analyzed by high-pressure liquid chromatography with a Coularray electrochemical detector from ESA Biosciences (Chelmsford, MA).

Statistical analysis

SPSS Statistics 25 (IBM Co., Armonk, NY) was used to perform all statistical analyses. One-way analysis of variance (ANOVA), followed by Student-Newman-Keul's test was used to test significance between multiple groups. Statistical analysis between two groups was performed with the Student's two-tailed t-test. If the data were not normally distributed, the Kruskal-Wallis test (non-parametric ANOVA) followed by Dunn's Multiple Comparison Test was used. We considered differences with values of $P < 0.05$ values to be statistically significant.

RESULTS

A caspase inhibitor and 4MP, but not NAC, protect against APAP nephrotoxicity.

To determine whether apoptosis was a relevant mechanism of cell death in the kidney, initial experiments utilized mice treated with a severe overdose of 600 mg/kg APAP for 24 h along with the water-soluble caspase inhibitor Ac-DEVD-CHO (3 mg/kg). In addition, animals were treated with either 50 mg/kg 4MP or 500 mg/kg NAC to compare protection with these interventions against APAP-induced hepatotoxicity and nephrotoxicity. Plasma ALT activity as an indicator of liver injury increased dramatically after APAP (Figure 1A). Treatment with NAC or 4MP effectively prevented the injury but the caspase inhibitor had no effect on elevated plasma ALT levels (Figure 1A) suggesting that liver injury was not due to apoptosis. In contrast, the increased levels of BUN, an indicator of kidney injury, due to APAP were not affected by NAC but reduced to baseline by 4MP and the caspase inhibitor (Figure 1B). Since it has been suggested that neutrophil gelatinase-associated lipocalin (NGAL) is a more reliable and sensitive biomarker of AKI as opposed to BUN and creatinine in animal and clinical studies (Medic et al., 2016; Schrezenmeier et al., 2017), we examined renal NGAL levels. Compared with the vehicle group, the group receiving APAP had significantly upregulated expression of NGAL protein in the kidney (Figure 1C). Pretreatment with Ac-DEVD-CHO almost completely prevented this increase in NGAL, reiterating the importance of caspase-mediated apoptosis in APAP-induced renal injury. Interestingly, treatment with 4MP also replicated the protection seen with caspase inhibitor, while NAC had no effect on the APAP-induced NGAL upregulation in the kidney (Figure 1D). These data demonstrate that Ac-DEVD-CHO selectively prevents kidney injury but has no effect on liver toxicity after an APAP overdose.

The histological evaluation confirmed the findings from the biomarkers with H&E staining demonstrating varying degrees of tubular injury including tubular dilation or rupture and brush border destruction in animals treated with APAP (Figure 2A). Apoptotic features were also evident in proximal tubular cell death as highlighted by distinct nuclear TUNEL staining (Figure 3A) when compared to the control tissue (Figure S1A). These histological features in the kidney caused by APAP overdose were significantly attenuated with both 4MP and Ac-DEVD-CHO treatments while NAC was not renal protective (Figures 2A, 3A). In contrast, APAP-induced severe liver injury as indicated by the extensive necrotic cell death (N) in the areas around the central veins (CV) (Figure 2B) accompanied by extensive nuclear DNA fragmentation that occurred in areas of necrosis characterized by diffuse TUNEL staining within the whole cell (Figure 3B). In contrast to the kidney, Ac-DEVD-CHO failed to protect against APAP-induced liver injury while NAC or 4MP treatments significantly reduced APAP-induced hepatic injury (Figures 2B, 3B). These histological data confirm disparate modes of cell death in the liver and kidney after an APAP overdose *in vivo* and suggest that Ac-DEVD-CHO has a potent role in protecting against APAP-induced apoptotic cell death, which exclusively occurs in the kidney's proximal tubules.

ER stress-associated caspase-12 dependent apoptosis in proximal tubular epithelial cells.

Although our data confirmed *in vivo* previous studies suggesting apoptotic cell death in isolated tubular epithelial cells (Lorz et al., 2005), the mechanistic reasons why APAP

induces apoptosis in the kidney and necrosis in the liver remain unclear. *In vitro* studies on murine proximal tubular epithelial cells revealed that APAP incubation can induce cell death with features of ER stress-mediated apoptosis without activation of the mitochondrial pathways as evidenced by the absence of cytosolic cytochrome c or Smac/DIABLO (Lorz et al., 2004). Thus, we explored whether this held true *in vivo* and whether it could explain the protection by 4MP in kidney cells after APAP. As shown in Figure 4A, 600 mg/kg APAP moderately increased the expression of ER stress markers such as PDI, and GRP78, in the kidney. This was significantly reduced by AC-DEVD-CHO pretreatment. Although AC-DEVD-CHO pretreatment induced a slight reduction of PDI and GRP78 expression, the additional ER stress marker, CHOP, was significantly decreased. Interestingly, 4MP also significantly reduced the expression of CHOP as opposed to NAC (Figure 4B,C), suggesting that ER stress-mediated apoptosis was involved in APAP nephrotoxicity *in vivo*. Caspase-12 is an ER-localized caspase that can be activated in response to sustained ER stress (Nakagawa et al, 2000). Our *in vivo* experiments revealed that APAP treatment did not affect procaspase-12 expression but enhanced procaspase-12 cleavage indicating its activation, which was again completely blocked by Ac-DEVD-CHO pretreatment (Figure 4A). Notably, caspase-12 cleavage products persisted in mice treated with APAP+NAC but were absent after 4MP cotreatment and pretreatment with Ac-DEVD-CHO (Figure 4A,D). These results, confirmed by densitometry analysis (Figure 4E), support the conclusion that the severe APAP overdose caused ER stress through the formation of protein adducts and triggered ER stress-mediated apoptotic cell death in the kidney *in vivo*, which can be effectively blocked by both 4MP and Ac-DEVD-CHO but not NAC.

4-MP inhibits microsomal and mitochondrial APAP protein adduct formation

APAP protein adduct formation is a critical mechanism of APAP-induced hepatic (Jollow et al., 1973) and also renal injury (Akakpo et al., 2020; Emeigh-Hart et al., 1991). To assess whether variance in the subcellular localization of APAP protein adducts may be driving differential cell death pathways in the kidney and the liver, we measured protein adducts in the ER and the mitochondria in both the kidney and the liver 4 h after APAP. The representative chromatograms in Figure 5 demonstrate that APAP-CYS can be detected in the liver (Figure 5A) and is significantly higher in the mitochondrial fraction compared to the ER (Figure 5B). Consistent with our previous report, APAP-CYS adducts peaks were almost undetectable in renal mitochondrial fractions while the levels were higher in the microsomal fraction (Figure 5A, B). Notably, 4MP effectively protected against adduct formation in the liver mitochondrial and microsomal fractions while also inhibiting adduct formation in renal microsomal fractions (Figure 5A, B). These results are consistent with the hypothesis that subcellular localization of protein adducts after APAP drives the mode of cell death, with mitochondrial adducts in the liver inducing mitochondrial dysfunction and necrotic cell death and ER adducts in the kidney causing ER stress and apoptosis. These data also indicate that 4MP protects against APAP nephrotoxicity by selectively inhibiting ER-localized Cyp2E1 in the kidney, which subsequently prevents protein adduct formation *in vivo* and thus blocks the induction of ER stress-mediated apoptotic cell death.

Cyp2E1 is selectively expressed in microsomes of proximal tubular epithelial cells.

Given the differential formation of APAP protein adducts in the kidney versus the liver, we investigated Cyp2E1 protein expression and its subcellular localization in both organs (Figure 6). We first localized Cyp2E1 in control liver and kidney tissue sections from C57BL/6J mice by immunohistochemistry staining (Figure 6A). Our data revealed that Cyp2E1 expression was predominantly localized in cells surrounding the central veins in the liver as shown earlier (Akakpo et al., 2022a; Umbaugh et al., 2021), while staining was predominantly seen in the cortex of the kidney (Figure 6A). Since the cortex is enriched in proximal tubular cells, we performed co-staining of Cyp2E1 and SGLT-2, a glucose transporter exclusively expressed in the renal proximal convoluted tubules (Figure 6B). The fluorescence staining signal of Cyp2E1 overlapped with the SGLT-2 signal confirming that renal proximal tubular cells are the primary cells expressing Cyp2E1 in the kidney. To further localize Cyp2E1 within subcellular compartments from the liver and kidney, we used a subcellular fractionation experimental approach of fresh tissue with western blot detection of Cyp2E1 protein levels in microsomal and mitochondrial fractions. This experiment revealed that while both the liver and the kidney tissues expressed Cyp2E1, only renal microsomal (Figure 6D) and not mitochondrial fractions (Figure 6 C,D) expressed Cyp2E1. We used β-actin as a loading control as this protein is present in most cellular compartments including mitochondria (Jayashankar and Rafelski, 2014) and microsomes (Pain et al., 2023). In contrast, the liver expressed CYP2E1 in both the mitochondria (Figure 6C) and the ER (Neve and Ingelman-Sundberg, 1999). These data indicate that in the kidney cortex, renal proximal tubular epithelial cells predominantly express Cyp2E1 in the ER where local production of APAP protein adducts initiates ER stress and apoptotic cell death. This contrasts with the liver, where despite Cyp2E1 localization to both the mitochondria and ER, adduct formation is significantly higher in the mitochondria (Figure 5B), which initiates distinct necrotic cell death pathways (Ramachandran and Jaeschke, 2019).

4MP protects against APAP-induced apoptotic cell death in primary human kidney cells

The next series of experiments evaluated whether the mechanism of APAP-induced kidney cell death we uncovered in the mouse *in vivo* is relevant for the human pathophysiology. As shown in Figure 7A, human kidney tissue expresses Cyp2E1, and co-staining of human kidney tissue with CYP2E1 and SGLT2 revealed that Cyp2E1 is also exclusively localized to the proximal tubular cells of human kidneys (Figure 7B). This is further reiterated in high-magnification images of isolated human primary kidney cells co-stained for Cyp2E1 and SGLT2 (Figure 8A). To test the susceptibility of human tubular cells to APAP, a dose-response treatment was performed in the isolated primary kidney cells (NHK). Exposure of NHK cells to APAP demonstrated a concentration-dependent loss of LDH with the 10 mM concentration causing the highest cell death at 24 h (Figure 8C,D) and 48 h (Figure 8D,E). Next, we evaluated the effects of 4MP, Ac-DEVD-CHO, and NAC after APAP treatment in NHK cells. Our data revealed that in the presence of 2 mM 4MP, or 20 μM Ac-DVED-CHO, APAP-induced cell death in these human kidney cells was significantly reduced with 4MP and completely prevented by the caspase inhibitor (Figure 9A,B). Analogous to the NAC effect in the mouse kidney, treating human cells with 20 mM NAC did not provide any protection against APAP-induced cell death. To determine whether reducing ER stress could alleviate caspase 12 activation and apoptosis, NHK cells were co-treated with

APAP and the molecular chaperone tauroursodeoxycholic acid (TUDCA), which is an ER stress inhibitor (Kusaczuk, 2019). Treating human cells with 100, 200 or 300 μM TUDCA provides significant protection against APAP-induced cell death (Figure 10A,B). These data indicate that 4MP and a caspase inhibitor but not NAC can have a protective role against APAP-induced acute kidney injury in primary human kidney cells.

DISCUSSION

Kidney damage in the context of APAP overdose has emerged as a clinically relevant problem (Akakpo et al., 2020; Blantz, 1996; Eguia and Materson, 1997; Hengy et al., 2009). Our previous analysis of a cohort of APAP overdose patients treated at the Banner-University Medical Center in Phoenix revealed no kidney dysfunction after moderate liver injury but severe liver injury in APAP overdose patients correlated with kidney dysfunction (Akakpo et al., 2020). Consistent with these clinical observations, we observed kidney injury only after a high overdose of APAP (600 mg/kg) but not after a moderate but still hepatotoxic overdose (300 mg/kg) (Akakpo et al., 2020). Therefore, studies of the mechanisms of kidney injury required the use of a high overdose. Investigation of the early mechanistic events in the kidney after an APAP overdose also indicated that while significant metabolism of APAP occurs in the kidney, mitochondrial adducts and c-Jun N-terminal kinase (JNK) activation were absent, in contrast to the liver (Akakpo et al., 2020). Importantly, NAC does not protect against APAP-induced nephrotoxicity suggesting that mechanisms of renal cell death are distinct from those of the liver (Jones and Vale, 1993; Slitt et al., 2004; Strehle and Haar, 2023). Previously, we investigated the effect of liposomal encapsulated GSH (control: free GSH) on recovering GSH levels after fasting in the liver, kidney and spleen (Wendel and Jaeschke, 1982). We showed that GSH administration (equivalent to Cys, Gly and Glu) can recover kidney GSH levels within 60 min clearly demonstrating that a supply of cysteine can stimulate GSH synthesis in the kidney. Thus, the kidney is clearly able to re-synthesize GSH in depleted tissue, but this may be under a different type of regulation than in the liver. Interestingly, clinical evidence indicates that while an APAP overdose can cause liver injury in patients, renal failure can also occur without liver failure (Campbell and Baylis, 1992; Eguia and Materson, 1997). However, the lack of liver failure does not preclude the occurrence of liver injury since the majority of APAP overdose patients recover after liver injury without developing liver failure. In any case, these effects observed in the clinic have not been replicated in animal models. In this paper, we demonstrate that Cyp2E1-mediated generation of NAPQI, protein adduct formation, and sustained ER stress induced by the severe APAP overdose are the principal events that trigger kidney injury. However, NAPQI can also bind to GSH to form APAP-GSH, and while important for the detoxification of NAPQI, APAP-GSH has also been implicated in the formation of a novel nephrotoxic compound (Stern et al., 2005). Another potential mechanism of renal toxicity is related to APAP bioactivation by prostaglandin endoperoxidase synthetase (PGES) in the medulla (Mugford and Tarloff, 1997). Together, an increase in these mechanisms may potentiate the development of kidney failure in patients without liver failure. These data emphasize the clinical relevance of better understanding the mechanisms of APAP-induced nephrotoxicity and the need to identify new therapeutic targets.

APAP-induced liver injury

In the liver, the injury process after an APAP overdose is initiated by the formation of NAPQI, which binds mitochondrial proteins (Ramachandran and Jaeschke, 2019). Mitochondrial dysfunction ensues due to inhibition of the electron transport chain and the formation of reactive oxygen species (Nguyen et al., 2021). Mitochondrial protein adduct and reactive oxygen generation are prerequisites for early activation of JNK (Nguyen et al., 2021). Then, phosphorylated JNK translocates to the mitochondria (Hanawa et al., 2008), which amplifies the mitochondrial oxidant stress and peroxynitrite formation (Saito et al., 2010) resulting in the induction of mitochondrial permeability transition pore (MPTP) opening (Kon et al., 2004). This triggers the release of mitochondrial intermembrane proteins like endonuclease G and AIF, which translocate to the nucleus to cause nuclear DNA fragmentation (Bajt et al., 2006). Importantly, several studies over the last decades have clearly demonstrated that APAP-induced liver damage is due to programmed necrosis (Iorga and Dara, 2019; Jaeschke et al., 2019) and that apoptosis does not play a relevant role after high or low overdoses of APAP in different strains of mice *in vivo* or in cultured mouse hepatocytes (Jaeschke et al., 2018). The lack of caspase activation and absence of hepatocellular apoptosis as observed in both fed and in fasted mice also indicates that this was not secondary necrosis (Gujral et al., 2002). In addition, no evidence of apoptosis was observed in primary human hepatocytes (Xie et al., 2014) or metabolically competent human HepaRG cells (McGill et al., 2011) after different doses of APAP. Furthermore, there was no apoptosis detectable in APAP overdose patients (McGill et al., 2012). Yet, it remains to be determined if the cascades of events primarily identified in the liver after an APAP overdose, also occur in the kidney.

APAP-induced kidney injury

Previous analysis of renal biopsies in patients with APAP toxicity and renal insufficiency have often described the occurrence of acute tubular epithelial cell necrosis (Blantz, 1996; Hengy et al., 2009; Eguia and Materson, 1997). Although tubular necrosis is seen in humans, that does not rule out early apoptosis, which subsequently evolves into necrosis (secondary necrosis) (Jaeschke and Lemasters, 2003). However, a key distinction between primary and secondary necrosis is the continued presence of caspase activation with secondary necrosis (Bajt et al., 2000). Apoptosis is a programmed form of cell death that may offer the opportunity for novel therapeutic interventions (Ortiz et al., 2001, 2003).

An alternative mitochondrial intrinsic pathway of apoptosis can be activated by DNA damage (Lossi, 2022). This pathway involves members of the Bcl-2 family that regulate mitochondrial Bax translocation and cytochrome c release. Recent studies have claimed that APAP causes mitochondrial dysfunction and mitochondrial-mediated apoptosis in the kidney, based solely on increased protein expression levels of pro-apoptotic genes like Bax, and caspase-3 as well as changes in expression of anti-apoptotic genes like Bcl-2 or mitochondrial membrane potential analysis (Shen et al., 2020; Wei et al., 2023). However, additional examination of the molecular mechanism of kidney damage revealed that the mitochondrial pathway was not activated during APAP-induced cell death as no loss of the mitochondrial membrane potential, as well as no mitochondrial Bax translocation or release of cytochrome c was detected *in vivo* (Lorz et al., 2005). In cultured murine

tubular epithelial cells, APAP triggered apoptosis through a caspase-mediated mechanism that involves caspase-9 and caspase-3 (Lorz et al., 2004). There was no mitochondrial release of cytochrome c and Smac/DIABLO while ER stress was suggested to mediate cell death in this *in vitro* study (Lorz et al., 2004). However, in mice, caspase-12 only localizes to the ER and has been implicated in an ER stress pathway that induces apoptosis (Nakagawa et al., 2000). In primary cultures of murine proximal tubular epithelial cells, APAP induced caspase-12 mediated apoptosis without mitochondrial dysfunction *in vitro* (Lorz et al., 2004). These data suggest that the intrinsic mitochondrial pathway is less likely to be involved in APAP-induced apoptosis in the kidney. Consistently, our *in vivo* data now demonstrate that APAP triggered an ER stress as indicated by CHOP, GRP78, and PDI induction as well as caspase-12 activation. The caspase inhibitor Ac-DEVD-CHO attenuated the ER stress, eliminated caspase-12 activation and kidney injury *in vivo,* and effectively prevented tubular cell death *in vitro*. In contrast to the kidney, Ac-DEVD-CHO did not affect liver injury, which is consistent with previous studies using moderate overdoses of APAP (Gujral et al., 2002). Importantly, 4MP also prevented caspase-12 activation and inhibited kidney injury *in vivo* and cell death in isolated renal epithelial cells. However, the standard of care for APAP overdose, NAC, did not prevent caspase-12 activation and kidney injury *in vivo* and in isolated human tubular cells even though this dose of NAC eliminated APAP-induced liver injury. However, the ER stress inhibitor, TUDCA, minimized cytotoxicity induced by APAP in NHK cells. This reinforces the important role of ER stress in the pathophysiology of APAP-induced apoptosis in the kidney. These data also suggest that APAP-induced liver and kidney injury are independent of each other, and that ER stress plays a key role in initiating APAP-induced kidney apoptotic cell death in a mouse model and in human renal tubular cells. These events are effectively counteracted by 4MP but not NAC.

Role of mitochondrial and microsomal Cyp2E1 in APAP toxicity in liver and kidney

The subcellular localization of Cyp2E1 in the mitochondria and microsomes has been demonstrated over several decades, with the first reports emerging in 1997 (Anandatheerthavarada et al., 1997). While most studies used a subcellular fractionation approach to detect Cyp2E1 expression in the liver (Neve and Ingelman-Sundberg, 1999, 2001), little is known about the subcellular localization of Cyp2E1 in the kidney. This is important since Cyp2E1-mediated metabolism of APAP has been implicated as a primary cause of AKI (Akakpo et al., 2020; Emeigh-Hart et al., 1991). After APAP overdose, the reactive metabolite, NAPQI, formed by Cyp2E1 in mice can bind covalently to cellular proteins to form APAP protein adducts in the kidney (Akakpo et al., 2020; Emeigh-Hart et al., 1991; Hart et al., 1994). This is a key event that triggers liver (Jollow et al., 1973; McGill et al., 2013) and kidney injury after an APAP overdose (Akakpo et al., 2020; Emeigh-Hart et al., 1991). However, we demonstrate that APAP adducts can only be formed in renal ER while both hepatic ER and mitochondria form adducts. Additionally, Cyp2E1 was mostly expressed in renal ER and not in renal mitochondria, unlike the liver, which expresses the enzyme in both organelles (Knockaert et al., 2011). This important finding is corroborated by an independent study that used immunogold EM to localize Cyp2E1 in ER and not in mitochondria of the kidney cells (Liu and Baliga, 2003). Procaspase-12 is expressed at high levels on the cytoplasmic side of the ER of renal tubular epithelial cells and can

be activated by sustained ER stress in mice (Hitomi et al., 2004; Nakagawa et al., 2000). Importantly, caspase-12 activates caspase-3, which is the executioner of apoptosis (Hitomi et al., 2004). This explains why Ac-DEVD-CHO, which is an effective caspase-3 inhibitor (Bajt et al., 2001), effectively protected against ER stress-mediated apoptosis in the kidney. It is worth noting that Ac-DEVD-CHO can also inhibit the activity of other caspases with lower efficiency (Boyle et al., 2013). Thus, ER stress induced by renal APAP metabolism of ER-localized Cyp2E1 is likely the primary event responsible for the initiation phase of an ER stress-induced apoptosis after a severe APAP overdose. These findings in mice using a 600 mg/kg dose of APAP are relevant for human patients, which also only show kidney dysfunction after severe injury caused by a high overdose of APAP (Akakpo et al., 2020).

N-acetylcysteine and 4-methylpyrazole in APAP-induced kidney injury

The current standard of care to treat APAP overdose patients is NAC, which has a limited therapeutic window (Rumack and Bateman, 2012) and does not protect against kidney toxicity in the mouse (Slitt et al., 2004), or in humans prompting the proposition of new guidelines for clinical use of NAC in patients following APAP overdose (Strehle and Haar, 2023). The study conducted herein further demonstrate that 4MP is superior to NAC at protecting human primary kidney cells against APAP-induced ER stress-mediated apoptotic cell death of proximal tubules. NAC is a membrane-permeable cysteine precursor that may passively (Pedre et al., 2021), but also actively (Hagos et al., 2017) deliver cysteine to kidney tubular cells. Interestingly, IP injection resulted in significant renal clearance of NAC by uptake and efflux transporters in mouse kidneys (Hagos et al., 2017). Thus, it remains to be determined whether the lack of renal protection in APAP-poisoned mice is due to an increased rate of NAC clearance after IP administration which may not adequately deliver NAC to renal tubules in the kidney. After free NAC enters a cell, it is rapidly hydrolyzed to release cysteine, which is the rate-limiting precursor of GSH synthesis. Moreover, NAC is a prodrug that requires the enzymatic cleavage of the acetyl group via the specific activity of the acylase to liberate free L-cysteine (Uttamsingh et al., 1998). An alternate prodrug of L-cysteine, Ribose Cysteine (Rib-Cys), can also deliver the amino acid to the cell by a non-enzymatic ring opening and solvolysis mechanism that differs from the NAC mechanism of action (Roberts et al., 1992). Interestingly, Rib-Cys protects against APAP-induced nephrotoxicity (Lucas et al., 2000; Slitt et al., 2005). Thus, further studies are needed to determine whether intracellular Acylase I activity in proximal tubular cells accounts for the greater efficacy of RibCys compared to NAC in renal protection against APAP toxicity. Together, the tissue-specific differences that exist between the liver and the kidney may be due to the membrane permeability and transport of NAC in renal cells, as well as the potential inability of renal cells to hydrolyze NAC and release L-Cysteine, which may, in turn, contribute to an altered GSH resynthesis pathway in renal cells. Importantly, Cyp2E1 activity in mitochondrial and microsomal fractions is higher in the liver than in the kidney, and its activity in the kidneys is higher in the ER than in mitochondria, where no relevant activity was detected (Arzuk et al., 2022). This low Cyp2E1 activity is due to the lack of Cyp2E1 localization to mitochondria which also explains the lack of renal APAP protein adduct formation in the mitochondria as opposed to the ER.

Summary and Conclusion

Treatment with a high overdose of APAP resulted in severe centrilobular necrosis in the liver and tubular cleavage of procaspase-12 and apoptosis in the kidney (Figure 11) . These findings are consistent with the fact that kidney dysfunction is only observed in patients with severe liver injury implying a high overdose of APAP (Akakpo et al., 2020). NAC protected against hepatic necrosis but could not prevent renal apoptosis (Figure 11). 4MP provided significant protection against renal APAP protein adduct formation, which was localized to the ER only. 4MP and Ac-DEVD-CHO significantly protected against APAP-induced ER stress and procaspase-12 activation while NAC did not. Our data indicate that the severe overdose of APAP led to sustained ER stress that is initiated by the Cyp2E1-mediated NAPQI and protein adduct formation in the ER, which triggers the cleavage and activation of procaspase-12, ultimately causing apoptotic cell death in the proximal tubular cells in the kidney.

Supplementary Material

Refer to Web version on PubMed Central for supplementary material.

ACKNOWLEDGEMENTS

This work was supported in part by National Institute of Diabetes and Digestive and Kidney Diseases (NIDDK) grants R01 DK102142 (HJ) and R01 DK125465 (AR) National Institute of General Medicine (NIGMS)-funded Liver Disease COBRE grants P20 GM103549 (HJ) and P30 GM118247 (HJ). This work was partly funded by a postdoctoral fellowship (J.Y.A.) from the CTSA grant funded by NCATS at the University of Kansas for Frontiers: University of Kansas Clinical and Translational Science Institute No. TL1TR002368. Primary cultures of human kidney cells were provided by the PKD Biomarkers and Biomaterials Core Laboratory in Kansas PKD Research and Translational Core Center (RTCC; NIH U54 DK126126) at KUMC and the national PKD Research Resource Consortium (PKD-RRC).

ABBREVIATIONS

AIF	apoptosis-inducing factor
AKI	acute kidney injury
ALF	acute liver failure
ALT	alanine aminotransferase
APAP	acetaminophen
BUN	blood urea nitrogen
CHOP	C/EBP Homologous Protein
Cyp2E1	cytochrome P450 2E1
ER	endoplasmic reticulum
GRP78	glucose regulated protein 78
GSH	glutathione

H&E	hematoxylin & eosin
JNK	c-Jun N-terminal kinase
MPTP	mitochondrial permeability transition pore
4MP	4-methylpyrazole
NAC	N-acetyl-L-cysteine
NAPQI	N-acetyl-p-benzoquinone imine
NGAL	neutrophil gelatinase-associated lipocalin
PDI	protein disulfide isomerase-A1
SGLT2	sodium-glucose cotransporter-2 (SGLT2)
Smac/DIABLO	Second Mitochondria-derived Activator of Caspases/Direct IAP-Binding protein with Low PI)
SOD	superoxide dismutase
TUNEL	terminal deoxynucleotidyl transferase-mediated dUTP nick end-labelling assay
TUDCA	Tauroursodeoxycholic acid

REFERENCES

Akakpo JY, Jaeschke MW, Etemadi Y, Artigues A, Toerber S, Olivos H, Shrestha B, Midey A, Jaeschke H, Ramachandran A, 2022a. Desorption Electrospray Ionization Mass Spectrometry Imaging Allows Spatial Localization of Changes in Acetaminophen Metabolism in the Liver after Intervention with 4-Methylpyrazole. J. Am. Soc. Mass Spectrom 33, 2094–2107. [PubMed: 36223142]

Akakpo JY, Jaeschke MW, Ramachandran A, Curry SC, Rumack BH, Jaeschke H, 2021. Delayed administration of N-acetylcysteine blunts recovery after an acetaminophen overdose unlike 4-methylpyrazole. Arch. Toxicol 95, 3377–3391. [PubMed: 34420083]

Akakpo JY, Ramachandran A, Curry SC, Rumack BH, Jaeschke H, 2022b. Comparing N-acetylcysteine and 4-methylpyrazole as antidotes for acetaminophen overdose. Arch. Toxicol 96, 453–465. [PubMed: 34978586]

Akakpo JY, Ramachandran A, Duan L, Schaich MA, Jaeschke MW, Freudenthal BD, Ding WX, Rumack BH, Jaeschke H, 2019. Delayed Treatment With 4-Methylpyrazole Protects Against Acetaminophen Hepatotoxicity in Mice by Inhibition of c-Jun n-Terminal Kinase. Toxicol. Sci 170, 57–68. [PubMed: 30903181]

Akakpo JY, Ramachandran A, Orhan H, Curry SC, Rumack BH, Jaeschke H, 2020. 4-methylpyrazole protects against acetaminophen-induced acute kidney injury. Toxicol. Appl. Pharmacol 409, 115317. [PubMed: 33157119]

Anandatheerthavarada HK, Addya S, Dwivedi RS, Biswas G, Mullick J, Avadhani NG, 1997. Localization of multiple forms of inducible cytochromes P450 in rat liver mitochondria: immunological characteristics and patterns of xenobiotic substrate metabolism. Arch. Biochem. Biophys 339, 136–150. [PubMed: 9056243]

Arzuk E, Tokdemir M, Orhan H, 2022. Mitochondrial versus microsomal bioactivation of paracetamol by human liver and kidney tissues. Toxicol. Lett 363, 36–44. [PubMed: 35595037]

Bajt ML, Cover C, Lemasters JJ, Jaeschke H, 2006. Nuclear translocation of endonuclease G and apoptosis-inducing factor during acetaminophen-induced liver cell injury. Toxicol. Sci 94, 217–225. [PubMed: 16896059]

Bajt ML, Knight TR, Lemasters JJ, Jaeschke H, 2004. Acetaminophen-induced oxidant stress and cell injury in cultured mouse hepatocytes: protection by N-acetylcysteine. Toxicol. Sci 80, 343–349. [PubMed: 15115886]

Bajt ML, Lawson JA, Vonderfecht SL, Gujral JS, Jaeschke H, 2000. Protection against Fas receptor-mediated apoptosis in hepatocytes and nonparenchymal cells by a caspase-8 inhibitor in vivo: evidence for a postmitochondrial processing of caspase-8. Toxicol. Sci 58, 109–117. [PubMed: 11053547]

Bajt ML, Vonderfecht SL, Jaeschke H, 2001. Differential protection with inhibitors of caspase-8 and caspase-3 in murine models of tumor necrosis factor and Fas receptor-mediated hepatocellular apoptosis. Toxicol. Appl. Pharmacol 175, 243–252. [PubMed: 11559023]

Blantz RC, 1996. Acetaminophen: acute and chronic effects on renal function. Am. J. Kidney Dis 28(Suppl 1), S3–6. [PubMed: 8669426]

Boyle AJ, Hwang J, Ye J, Shih H, Jun K, Zhang Y, Fang Q, Sievers R, Yeghiazarians Y, Lee RJ, 2013. The effects of aging on apoptosis following myocardial infarction. Cardiovasc. Ther 31, e102–10. [PubMed: 24279384]

Campbell NR, Baylis B, 1992. Renal impairment associated with an acute paracetamol overdose in the absence of hepatotoxicity. Postgrad. Med. J 68, 116–118. [PubMed: 1570251]

Eguia L, Materson BJ, 1997. Acetaminophen-related acute renal failure without fulminant liver failure. Pharmacotherapy 17, 363–370. [PubMed: 9085330]

Emeigh Hart SG, Birge RB, Cartun RW, Tyson CA, Dabbs JE, Nishanian EV, Wyand DS, Khairallah EA, Cohen SD, 1991. In vivo and in vitro evidence for in situ activation and selective covalent binding of acetaminophen (APAP) in mouse kidney. Adv. Exp. Med. Biol 283, 711–716. [PubMed: 2069045]

Fisher ES, Curry SC, 2019. Evaluation and treatment of acetaminophen toxicity. Adv. Pharmacol 85, 263–272. [PubMed: 31307590]

Gujral JS, Knight TR, Farhood A, Bajt ML, Jaeschke H, 2002. Mode of cell death after acetaminophen overdose in mice: apoptosis or oncotic necrosis? Toxicol. Sci 67: 322–328. [PubMed: 12011492]

Gyrd-Hansen M, Farkas T, Fehrenbacher N, Bastholm L, Høyer-Hansen M, Elling F, Wallach D, Flavell R, Kroemer G, Nylandsted J, Jäättelä M, 2006. Apoptosome-independent activation of the lysosomal cell death pathway by caspase-9. Mol. Cell. Biol 26, 7880–78891. [PubMed: 16966373]

Hagos FT, Daood MJ, Ocque JA, Nolin TD, Bayir H, Poloyac SM, Kochanek PM, Clark RS, Empey PE, 2017. Probenecid, an organic anion transporter 1 and 3 inhibitor, increases plasma and brain exposure of N-acetylcysteine. Xenobiotica 47, 346–353. [PubMed: 27278858]

Hanawa N, Shinohara M, Saberi B, Gaarde WA, Han D, Kaplowitz N, 2008. Role of JNK translocation to mitochondria leading to inhibition of mitochondria bioenergetics in acetaminophen-induced liver injury. J. Biol. Chem 283, 13565–13577. [PubMed: 18337250]

Hart SG, Beierschmitt WP, Wyand DS, Khairallah EA, Cohen SD, 1994. Acetaminophen nephrotoxicity in CD-1 mice. I. Evidence of a role for in situ activation in selective covalent binding and toxicity. Toxicol. Appl. Pharmacol 126, 267–275. [PubMed: 8209379]

Hart SG, Cartun RW, Wyand DS, Khairallah EA, Cohen SD, 1995. Immunohistochemical localization of acetaminophen in target tissues of the CD-1 mouse: correspondence of covalent binding with toxicity. Fundam. Appl. Toxicol 24, 260–274. [PubMed: 7737437]

Hengy B, Hayi-Slayman D, Page M, Christin F, Baillon JJ, Ber CE, Allaouchiche B, Rimmelé T, 2009. [Acute renal failure after acetaminophen poisoning: report of three cases]. Can. J. Anaesth 56, 770–774. [PubMed: 19639374]

Hitomi J, Katayama T, Taniguchi M, Honda A, Imaizumi K, Tohyama M, 2004. Apoptosis induced by endoplasmic reticulum stress depends on activation of caspase-3 via caspase-12. Neurosci. Lett 357, 127–130. [PubMed: 15036591]

Hodgman MJ, Garrard AR, 2012. A review of acetaminophen poisoning. Crit. Care Clin 28, 499–516. [PubMed: 22998987]

Hu JJ, Rhoten WB, Yang CS, 1990. Mouse renal cytochrome P450IIE1: immunocytochemical localization, sex-related difference and regulation by testosterone. Biochem. Pharmacol 40, 2597–2602. [PubMed: 2260985]

Iorga A, Dara L, 2019. Cell death in drug-induced liver injury. Adv. Pharmacol 85, 31–74. [PubMed: 31307591]

Jaeschke H., 2015. Acetaminophen: Dose-Dependent Drug Hepatotoxicity and Acute Liver Failure in Patients. Dig. Dis 33, 464–471. [PubMed: 26159260]

Jaeschke H, Duan L, Akakpo JY, Farhood A, Ramachandran A, 2018. The role of apoptosis in acetaminophen hepatotoxicity. Food Chem. Toxicol 118, 709–718. [PubMed: 29920288]

Jaeschke H, Lemasters JJ, 2003. Apoptosis versus oncotic necrosis in hepatic ischemia/reperfusion injury. Gastroenterology 125, 1246–1257. [PubMed: 14517806]

Jaeschke H, Ramachandran A, Chao X, Ding WX, 2019. Emerging and established modes of cell death during acetaminophen-induced liver injury. Arch Toxicol 93, 3491–3502. [PubMed: 31641808]

Jayashankar V, Rafelski SM, 2014. Integrating mitochondrial organization and dynamics with cellular architecture. Curr. Opin. Cell. Biol 26, 34–40. [PubMed: 24529244]

Jollow DJ, Mitchell JR, Potter WZ, Davis DC, Gillette JR, Brodie BB, 1973. Acetaminophen-induced hepatic necrosis. II. Role of covalent binding in vivo. J. Pharmacol. Exp. Ther 187, 195–202. [PubMed: 4746327]

Jones AF, Vale JA, 1993. Paracetamol poisoning and the kidney. J Clin Pharm Ther 18, 5–8. [PubMed: 8473360]

Knockaert L, Fromenty B, Robin MA 2011. Mechanisms of mitochondrial targeting of cytochrome P450 2E1: pathophysiological role in liver injury and obesity. FEBS J. 278, 4252–4260. [PubMed: 21929725]

Kon K, Kim JS, Jaeschke H, Lemasters JJ, 2004. Mitochondrial permeability transition in acetaminophen-induced necrosis and apoptosis of cultured mouse hepatocytes. Hepatology 40, 1170–1179. [PubMed: 15486922]

Kusaczuk M., 2019. Tauroursodeoxycholate-Bile Acid with Chaperoning Activity: Molecular and Cellular Effects and Therapeutic Perspectives. Cells 8, 1471. [PubMed: 31757001]

Liu H, Baliga R, 2003. Cytochrome P450 2E1 null mice provide novel protection against cisplatin-induced nephrotoxicity and apoptosis. Kidney Int. 63, 1687–1696. [PubMed: 12675844]

Lorz C, Justo P, Sanz AB, Egido J, Ortíz A, 2005. Role of Bcl-xL in paracetamol-induced tubular epithelial cell death. Kidney Int. 67, 592–601. [PubMed: 15673306]

Lorz C, Justo P, Sanz A, Subirá D, Egido J, Ortiz A, 2004. Paracetamol-induced renal tubular injury: a role for ER stress. J. Am. Soc. Nephrol 15, 380–389. [PubMed: 14747384]

Lossi L., 2022. The concept of intrinsic versus extrinsic apoptosis. Biochem. J 479, 357–384. [PubMed: 35147165]

Lucas AM, Hennig G, Dominick PK, Whiteley HE, Roberts JC, Cohen SD, 2000. Ribose cysteine protects against acetaminophen-induced hepatic and renal toxicity. Toxicol. Pathol 28, 697–704. [PubMed: 11026606]

Mazer M, Perrone J, 2008. Acetaminophen-induced nephrotoxicity: pathophysiology, clinical manifestations, and management. J. Med. Toxicol 4, 2–6. [PubMed: 18338302]

McClain CJ, Holtzman J, Allen J, Kromhout J, Shedlofsky S, 1988. Clinical features of acetaminophen toxicity. J. Clin. Gastroenterol 10, 76–80. [PubMed: 3356889]

McGill MR, Lebofsky M, Norris HR, Slawson MH, Bajt ML, Xie Y, Williams CD, Wilkins DG, Rollins DE, Jaeschke H, 2013. Plasma and liver acetaminophen-protein adduct levels in mice after acetaminophen treatment: dose-response, mechanisms, and clinical implications. Toxicol. Appl. Pharmacol 269, 240–249. [PubMed: 23571099]

McGill MR, Sharpe MR, Williams CD, Taha M, Curry SC, Jaeschke H, 2012. The mechanism underlying acetaminophen-induced hepatotoxicity in humans and mice involves mitochondrial damage and nuclear DNA fragmentation. J. Clin. Invest 122, 1574–1583. [PubMed: 22378043]

McGill MR, Yan HM, Ramachandran A, Murray GJ, Rollins DE, Jaeschke H, 2011. HepaRG cells: a human model to study mechanisms of acetaminophen hepatotoxicity. Hepatology 53, 974–982. [PubMed: 21319200]

McMartin KE, 2010. Antidotes for alcohol and glycol toxicity: translating mechanisms into treatments. Clin. Pharmacol. Ther 88, 400–404. [PubMed: 20686479]

Medic B, Rovcanin B, Vujovic KS, Obradovic D, Duric D, Prostran M, 2016. Evaluation of Novel Biomarkers of Acute Kidney Injury: The Possibilities and Limitations. Curr. Med. Chem 23, 1981–1997. [PubMed: 26860999]

Mour G, Feinfeld DA, Caraccio T, McGuigan M, 2005. Acute renal dysfunction in acetaminophen poisoning. Ren. Fail 27, 381–383. [PubMed: 16060123]

Mugford CA, Tarloff JB, 1997. The contribution of oxidation and deacetylation to acetaminophen nephrotoxicity in female Sprague-Dawley rats. Toxicol. Lett 93, 15–22. [PubMed: 9381478]

Nakagawa T,, Zhu H, Morishima N, Li E, Xu J, Yankner BA, Yuan J, 2000. Caspase-12 mediates endoplasmic-reticulum-specific apoptosis and cytotoxicity by amyloid-beta. Nature 403, 98–103. [PubMed: 10638761]

Neve EP, Ingelman-Sundberg M, 1999. A soluble NH(2)-terminally truncated catalytically active form of rat cytochrome P450 2E1 targeted to liver mitochondria. FEBS Lett. 460, 309–314. [PubMed: 10544255]

Neve EP, Ingelman-Sundberg M, 2002. Identification and characterization of a mitochondrial targeting signal in rat cytochrome P450 2E1 (CYP2E1). J. Biol. Chem 276, 11317–11322.

Nguyen NT, Du K, Akakpo JY, Umbaugh DS, Jaeschke H, Ramachandran A, 2021. Mitochondrial protein adduct and superoxide generation are prerequisites for early activation of c-jun N-terminal kinase within the cytosol after an acetaminophen overdose in mice. Toxicol. Lett 338, 21–31. [PubMed: 33290831]

Ortiz A, Justo P, Sanz A, Lorz C, Egido J, 2003. Targeting apoptosis in acute tubular injury. Biochem. Pharmacol 66, 1589–1594. [PubMed: 14555238]

Ortiz A, Lorz C, Justo P, Catalán MP, Egido J, 2001. Contribution of apoptotic cell death to renal injury. J. Cell. Mol. Med 5, 18–32. [PubMed: 12067448]

Pain C, Tolmie F, Wojcik S, Wang P, Kriechbaumer V, 2023. intER-ACTINg: The structure and dynamics of ER and actin are interlinked. J. Microsc 291, 105–118. [PubMed: 35985796]

Pedre B, Barayeu U, Ezerina D, Dick TP, 2021. The mechanism of action of N-acetylcysteine (NAC): The emerging role of H(2)S and sulfane sulfur species. Pharmacol. Ther 228, 107916. [PubMed: 34171332]

Ramachandran A, Jaeschke H, 2019. Acetaminophen Hepatotoxicity. Semin. Liver Dis 39, 221–234. [PubMed: 30849782]

Roberts JC, Charyulu RL, Zera RT, Nagasawa HT, 1992. Protection against acetaminophen hepatotoxicity by ribose-cysteine (RibCys). Pharmacol. Toxicol 70, 281–285. [PubMed: 1608914]

Rumack BH, Bateman DN, 2012. Acetaminophen and acetylcysteine dose and duration: past, present and future. Clin. Toxicol. (Phila) 50, 91–98. [PubMed: 22320209]

Saito C, Lemasters JJ, Jaeschke H, 2010. c-Jun N-terminal kinase modulates oxidant stress and peroxynitrite formation independent of inducible nitric oxide synthase in acetaminophen hepatotoxicity. Toxicol. Appl. Pharmacol 246, 8–17. [PubMed: 20423716]

Schrezenmeier EV, Barasch J, Budde K, Westhoff T, Schmidt-Ott KM, 2017. Biomarkers in acute kidney injury - pathophysiological basis and clinical performance. Acta Physiol. (Oxf) 219, 554–572. [PubMed: 27474473]

Shen Y, Jin X, Chen W, Gao C, Bian Q, Fan J, Luan J, Cao Z, Guo Z, Gu Y, Liu H, Ju D, Mei X, 2020. Interleukin-22 ameliorated acetaminophen-induced kidney injury by inhibiting mitochondrial dysfunction and inflammatory responses. Appl. Microbiol. Biotechnol 104, 5889–5898. [PubMed: 32356198]

Slitt AL, Dominick PK, Roberts JC, Cohen SD, 2004. Standard of care may not protect against acetaminophen-induced nephrotoxicity. Basic Clin. Pharmacol. Toxicol 95, 247–248. [PubMed: 15546480]

Slitt AM, Dominick PK, Roberts JC, Cohen SD, 2005. Effect of ribose cysteine pretreatment on hepatic and renal acetaminophen metabolite formation and glutathione depletion. Basic Clin. Pharmacol. Toxicol 96, 487–494. [PubMed: 15910414]

Stern ST, Bruno MK, Horton RA, Hill DW, Roberts JC, Cohen SD, 2005. Contribution of acetaminophen-cysteine to acetaminophen nephrotoxicity II. Possible involvement of the gamma-glutamyl cycle. Toxicol. Appl. Pharmacol 202, 160–171. [PubMed: 15629191]

Strehle EM, Haar I, 2023. Acute kidney injury after treatment of paracetamol overdose using new N-acetylcysteine guideline. Arch. Dis. Child 108, 416–417. [PubMed: 36822838]

Tujios SR, Hynan LS, Vazquez MA, Larson AM, Seremba E, Sanders CM, Lee WM; Acute Liver Failure Study Group., 2015. Risk factors and outcomes of acute kidney injury in patients with acute liver failure. Clin. Gastroenterol. Hepatol 13, 352–359. [PubMed: 25019700]

Umbaugh DS, Ramachandran A, Jaeschke H, 2021. Spatial Reconstruction of the Early Hepatic Transcriptomic Landscape After an Acetaminophen Overdose Using Single-Cell RNA-Sequencing. Toxicol. Sci 182, 327–345. [PubMed: 33983442]

Uttamsingh V, Keller DA, Anders MW, 1998. Acylase I-catalyzed deacetylation of N-acetyl-L-cysteine and S-alkyl-N-acetyl-L-cysteines. Chem. Res. Toxicol 11, 800–809. [PubMed: 9671543]

Wallace DP, Reif GA, 2019. Generation of primary cells from ADPKD and normal human kidneys. Methods Cell Biol. 153, 1–23. [PubMed: 31395374]

Wei M, Gao Y, Cheng D, Zhang H, Zhang W, Shen Y, Huang Q, An X, Wang B, Yu Z, Wang N, Chen H, Xu Y, Gui D, 2023. Notoginsenoside Fc ameliorates renal tubular injury and mitochondrial damage in acetaminophen-induced acute kidney injury partly by regulating SIRT3/SOD2 pathway. Front. Med. (Lausanne) 9, 1055252. [PubMed: 36714147]

Wendel A, Jaeschke H, 1982. Drug-induced lipid peroxidation in mice--III. Glutathione content of liver, kidney and spleen after intravenous administration of free and liposomally entrapped glutathione. Biochem. Pharmacol 31, 3607–3611. [PubMed: 7181941]

Xie Y, McGill MR, Dorko K, Kumer SC, Schmitt TM, Forster J, Jaeschke H, 2014. Mechanisms of acetaminophen-induced cell death in primary human hepatocytes. Toxicol. Appl. Pharmacol 279, 266–274. [PubMed: 24905542]

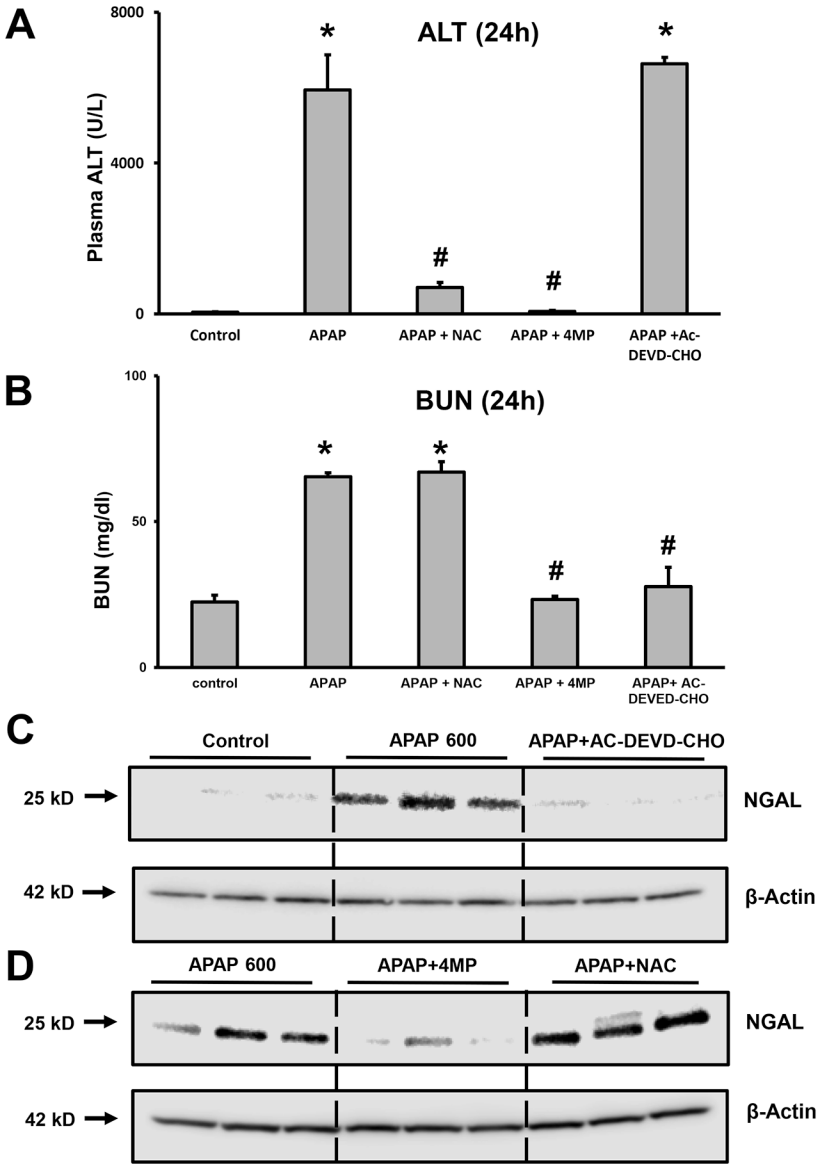

Figure 1: Effect of inhibition of apoptosis on renal and hepatic injury after a severe APAP overdose.

C57BL/6J mice were treated with 600 mg/kg APAP and sacrificed after 24 h for the collection of blood and tissues. Groups of mice also received a co-treatment with 50 mg/kg 4MP, 500 mg/kg NAC, or 3 mg/kg Ac-DVED-CHO. Graphs are means ± SEM for plasma ALT activities (A) and Blood Urea Nitrogen (BUN) levels (B); n= 8 animals per group. *P< 0.05 (compared to control). #P<0.05 (compared to APAP). Kidney homogenates were subjected to western blotting for NGAL and β-actin (C) and (D). Samples are from 3 representative animals per group.

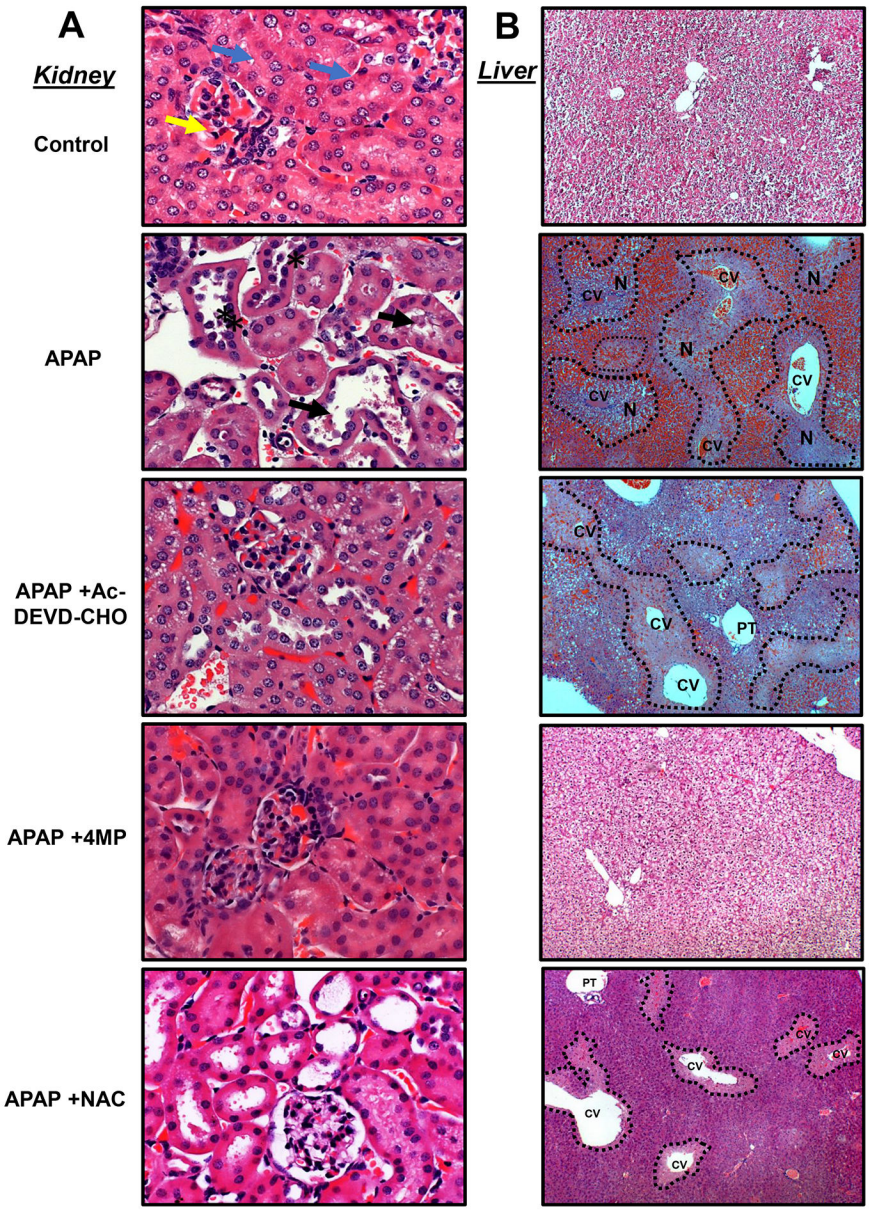

Figure 2: Effect of apoptosis inhibition on kidney and liver histology.

Mice were treated with 600 mg/kg APAP or saline (10 ml/kg) by intraperitoneal (IP) injection. Then, mice received an IP cotreatment of 50 mg/kg 4MP, 500 mg/kg NAC, 3 mg/kg Ac-DEVD-CHO, or vehicle. Mice were killed 24 h after APAP. Tissue sections were stained for H&E to visualize kidney and liver morphology. Representative images of H&E staining of kidney sections (right panels) in control show normal renal corpuscle, glomerulus, and bowman's capsule (yellow arrow) surrounded with intact tubules that are lined with high cuboidal cells having rounded nuclei (blue arrow). In contrast, tissue from APAP-dosed mice shows dilated intertubular cortical blood vessels dilated tubules, rupture of brush border, and tubular necrosis (black star) with the accumulation of necrotic debris within the collecting tubules (black arrow) (black arrowhead) (A) (x200). Representative images of H&E staining of liver sections (left panels) are shown in control with normal

hepatocytes filled with glycogen. In contrast, liver tissue from APAP-dosed mice displayed dilation of central veins (CV) surrounding the portal triad (PT) and accumulation of red blood cells. Centrilobular necrosis of the hepatocytes is highlighted in the image with a dashed line (B) (x100). Representative image from 8 animals per group.

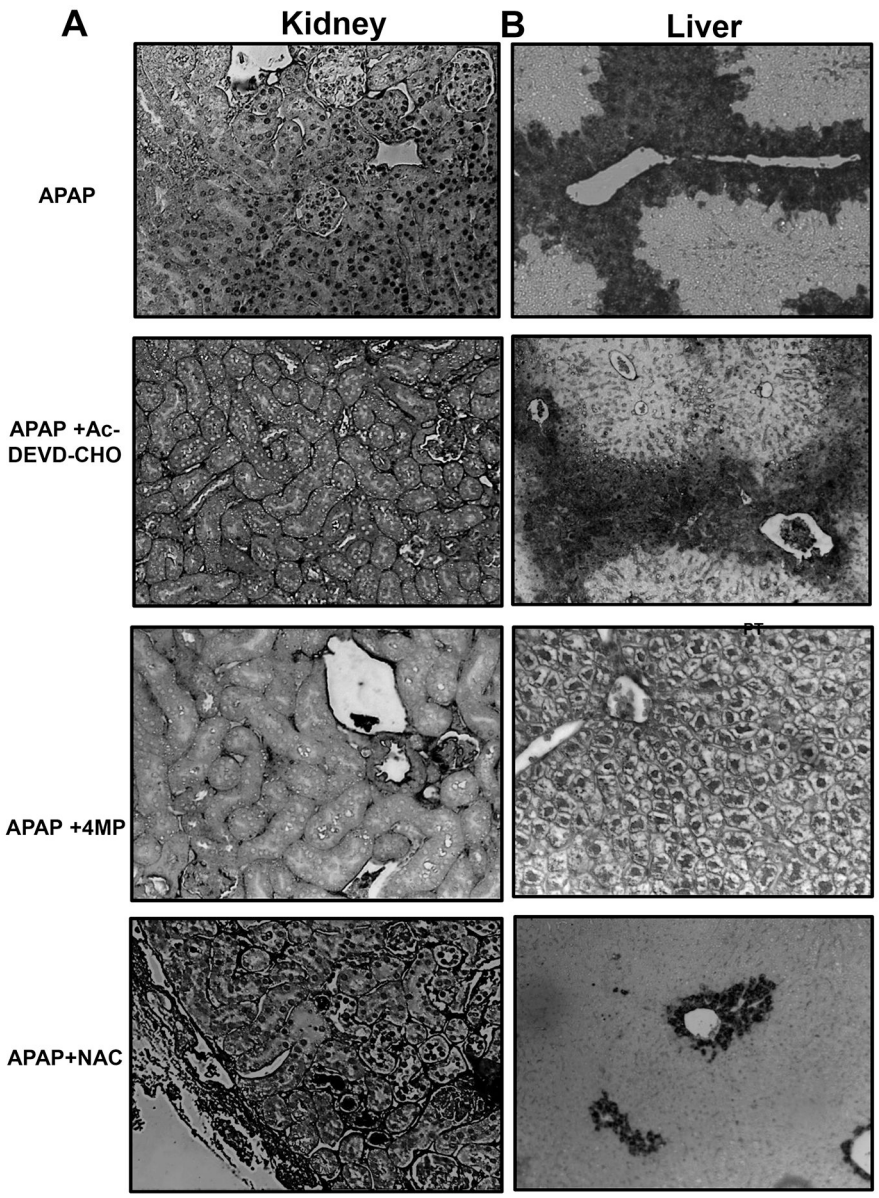

Figure 3: Effect of Ac-DEVD-CHO on apoptotic cell death in the kidney and necrotic cell death in the liver.

Mice were treated with 600 mg/kg APAP or saline (10 ml/kg) by intraperitoneal injection for 24 h. Then, mice received an IP co-treatment of 50 mg/kg 4MP, 500 mg/kg NAC or 3 mg/kg Ac-DEVD-CHO. Representative TUNEL images of the kidney (left panels) showing distinct nuclear TUNEL staining that are present in the APAP and APAP + NAC group but absent in the APAP +Ac-DEVD-CHO and APAP +NAC group (A). Representative TUNEL images of liver tissue (right panels) highlighting extensive nuclear DNA fragmentation that occurred in areas of necrosis present in all groups but APAP +4MP (B) (all x100) stained with TUNEL assay. Representative image from 8 animals per group.

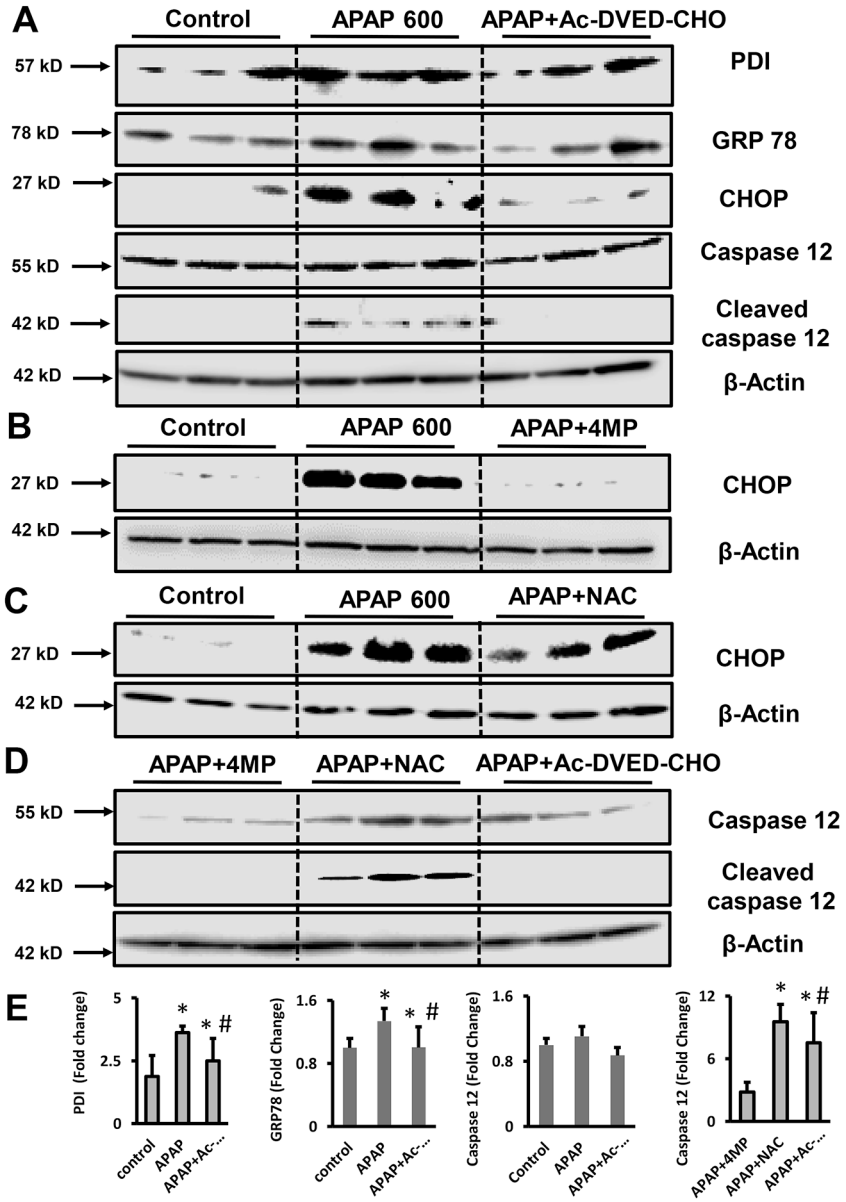

Figure 4: ER stress and ER-mediated apoptosis in the kidney after APAP overdose.

Mice were treated with 600 mg/kg APAP or saline (10 ml/kg) IP for 24 h. Then, mice received a co-treatment of 50 mg/kg 4MP, 500 mg/kg NAC, or 3 mg/kg Ac-DEVD-CHO IP. PDI, GRP78, CHOP, caspase-12, and cleaved caspase-12 protein expression was assessed by western blot in kidney tissue homogenate at 24 h between control, APAP, and Ac-DEVD-CHO treatment (A), in controls, APAP and APAP+4MP treated animals (B), after control, APAP, and APAP+NAC (C) treatment and after APAP+4MP, APAP+NAC and Ac-DEVD-CHO treatments (D). Samples are from 3 representative animals per group. *P < 0.05 (compared with control). #P < 0.05 (compared with APAP).

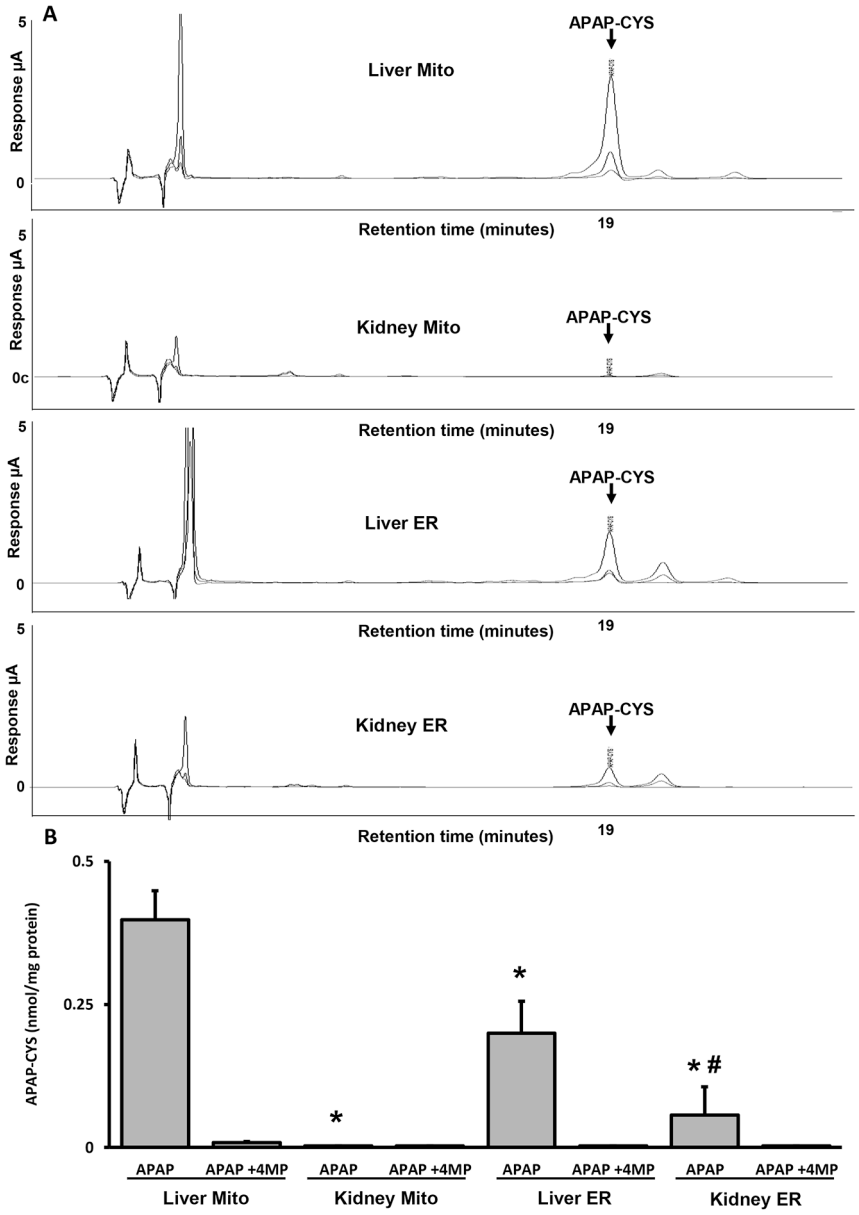

Figure 5: Mitochondrial versus endoplasmic APAP protein adducts.

Mice were treated with 600 mg/kg APAP alone or with 50 mg/kg 4MP for 4 h. (A) Representative chromatogram of APAP protein adducts in different subcellular fractions. Traces indicate the 3 different potentials set at 180, 280, and 300 mV on the Coularray electrochemical detector. (B) APAP protein adducts in the ER and in mitochondria. Data represent means ± SEM of 3 measurements per preparation (n = 6 animals per group). *P < 0.05 (compared with liver mitochondrial fraction). #P < 0.05 (compared with kidney mitochondrial fraction). Statistical comparisons (* and #) are with the APAP group.

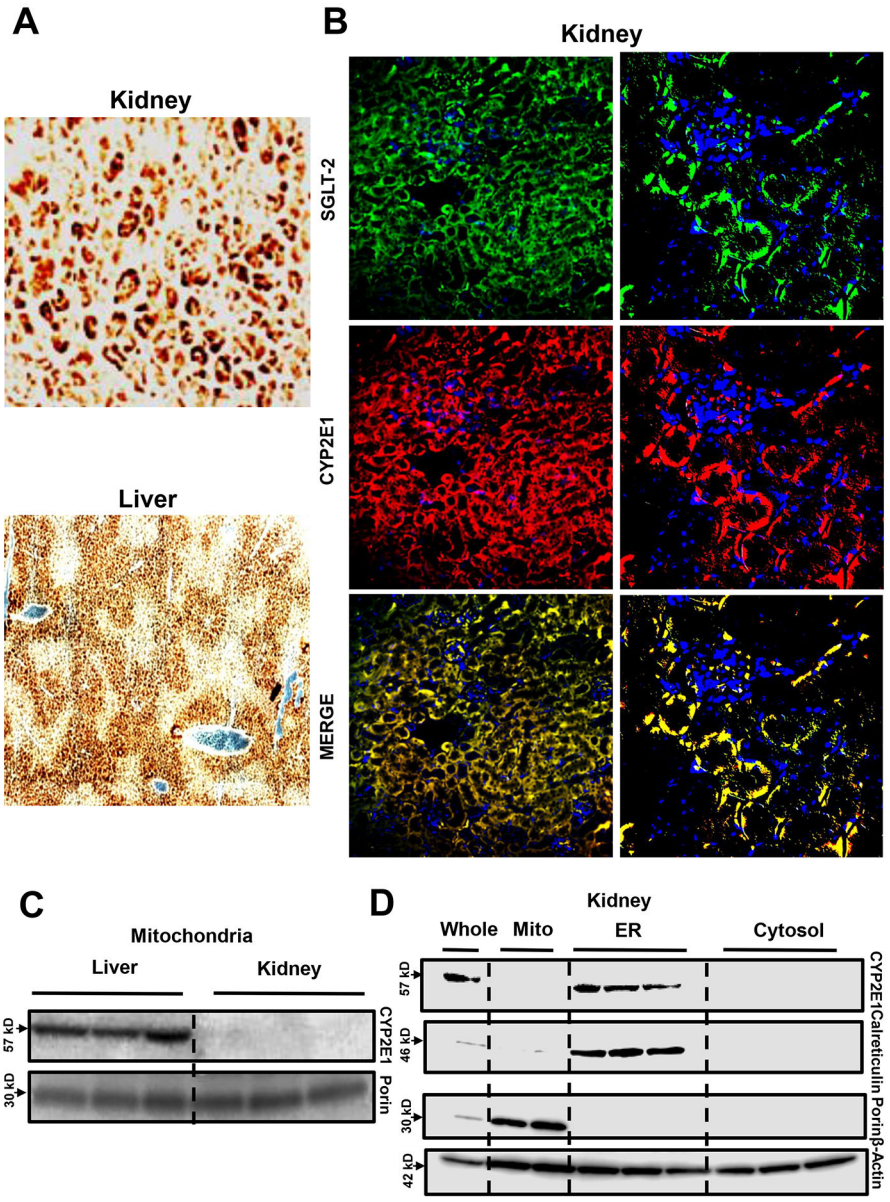

Figure 6: Cyp2E1 expression in mouse liver and kidney.

Immunohistochemistry of Cyp2E1 in the kidney and the liver (A) (x200). Co-staining of SGLT-2 and Cyp2E1 on kidney tissue sections of control mice (magnification: x200 on the left and x600 on the right) (B). Kidney (C, D) and liver (C) homogenates from untreated mice were subjected to western blot analysis to assess subcellular expression of Cyp2E1. Representative image from 3 animals per group. Western blot samples are from 3 representative animals per group.

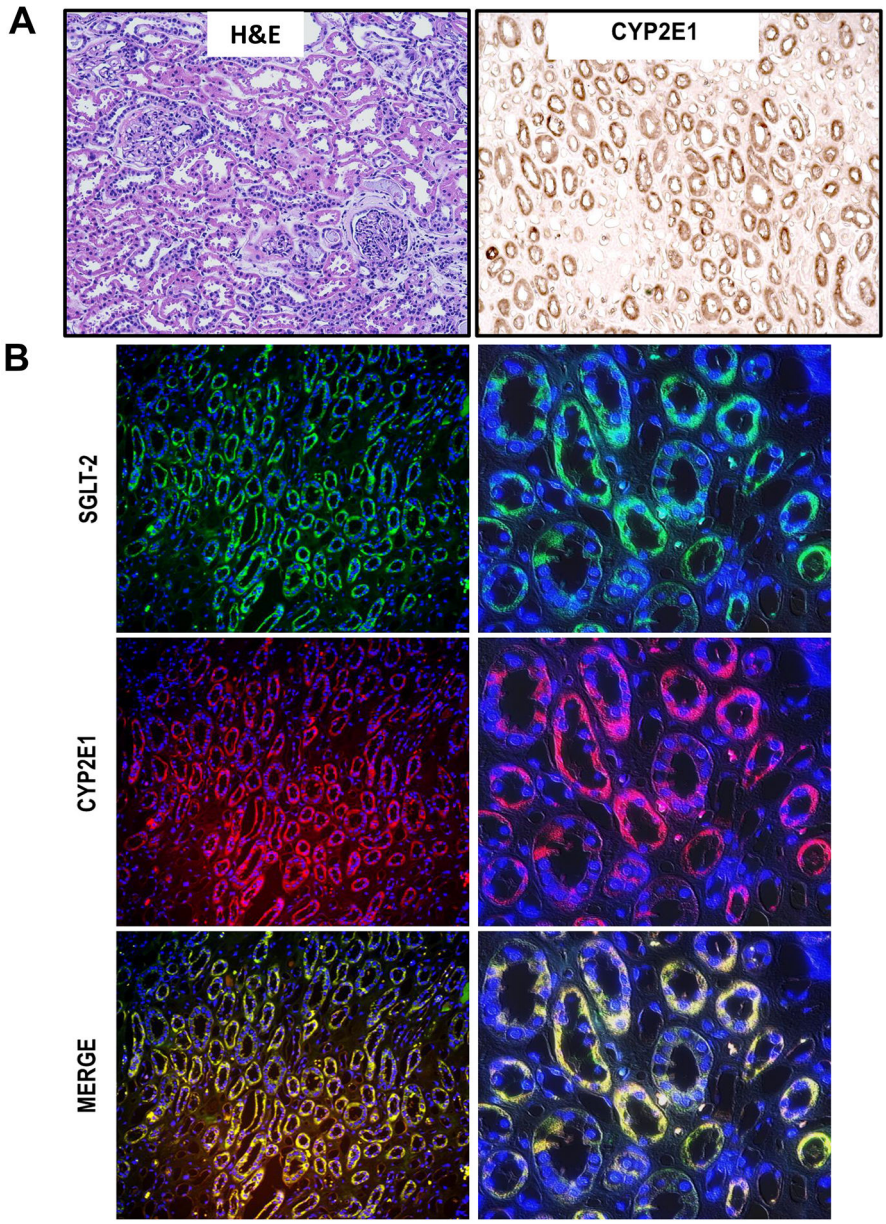

Figure 7: Renal Cyp2E1 expression in the kidney of human tissue sections.

H&E and immunohistochemistry of Cyp2E1 in the kidney (A) (x200). Immunofluorescence co-staining of SGLT-2 and Cyp2E1 on kidney sections (magnification: x200 on the left and x600 on the right) (B). Representative image from 3 male donors per group.

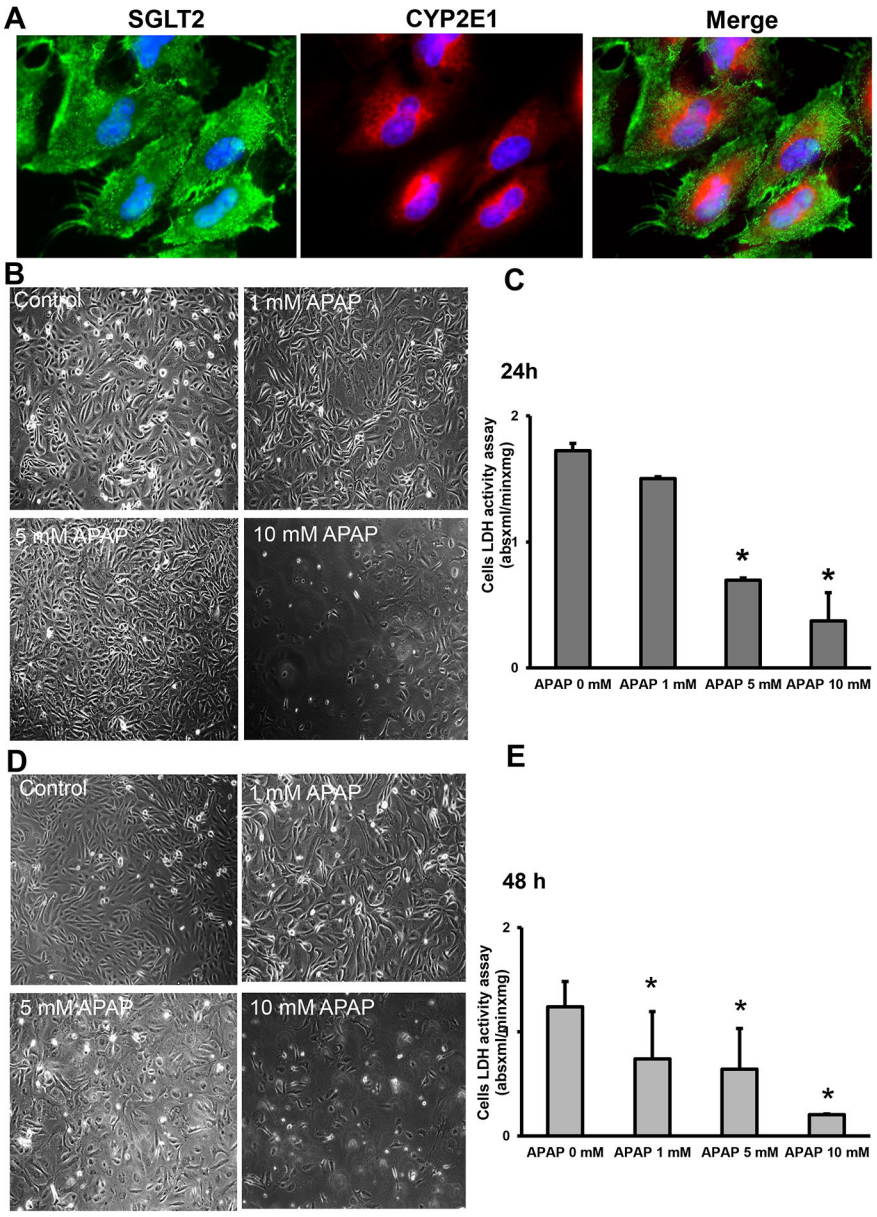

Figure 8: Susceptibility of primary normal human kidney (NHK) cells to APAP.

Cells were treated with 1 to 10 mM of APAP for 24 or 48 h. Immunofluorescence co-staining of SGLT-2 and Cyp2E1 on kidney section (x600 magnification) (A). Phase contrast images of control and APAP-treated cells at 24 h (B) (x200). Dose-dependent LDH activity in cells at 24 h (C). Phase contrast images of control and treated cells at 48 h (B) (x200). Dose-dependent LDH activity in cells at 48 h (C). Bars represent means ± SEM for three separate treatments. *P < 0.05 versus control

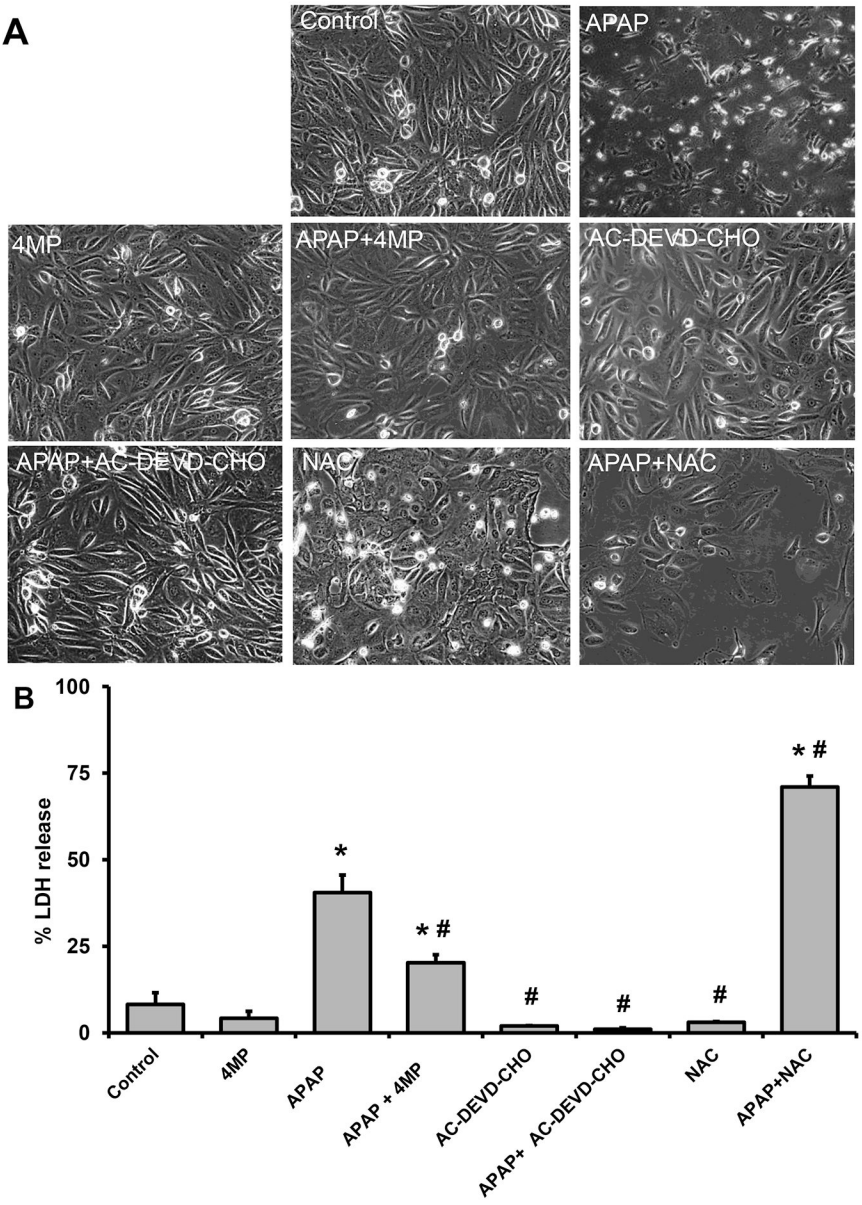

Figure 9: Effect of 4MP, Ac-DEVD-CHO, and NAC in APAP-treated NHK cells.

Cells were treated with 10 mM APAP alone or in combination with 2 mM 4MP, 20 mM NAC, or 20 μM Ac-DEVD-CHO. Phase contrast images of control and treated cells (A) (x200). % LDH release into the culture medium. Bars represent means ± SEM for three separate experiments. *P < 0.05 versus control; #P < 0.05 versus APAP.

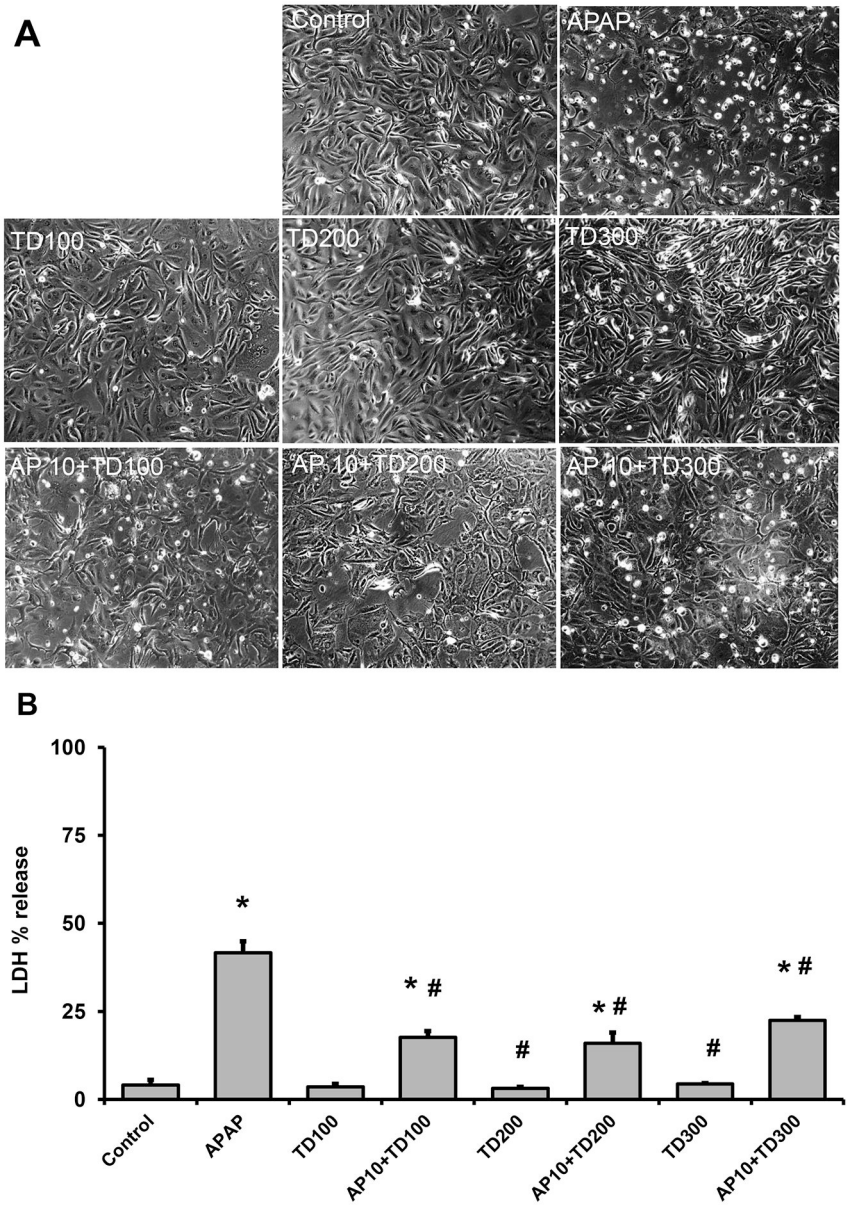

Figure 10: Effect of TUDCA in APAP-treated NHK cells.

Cells were treated with 10 mM APAP alone or in combination with 100, 200, or 300 μM TUDCA. Phase contrast images of control and treated cells (A) (x200). % LDH release into the culture medium (B). Bars represent means ± SEM for three separate experiments. *P < 0.05 versus control; #P < 0.05 versus APAP.

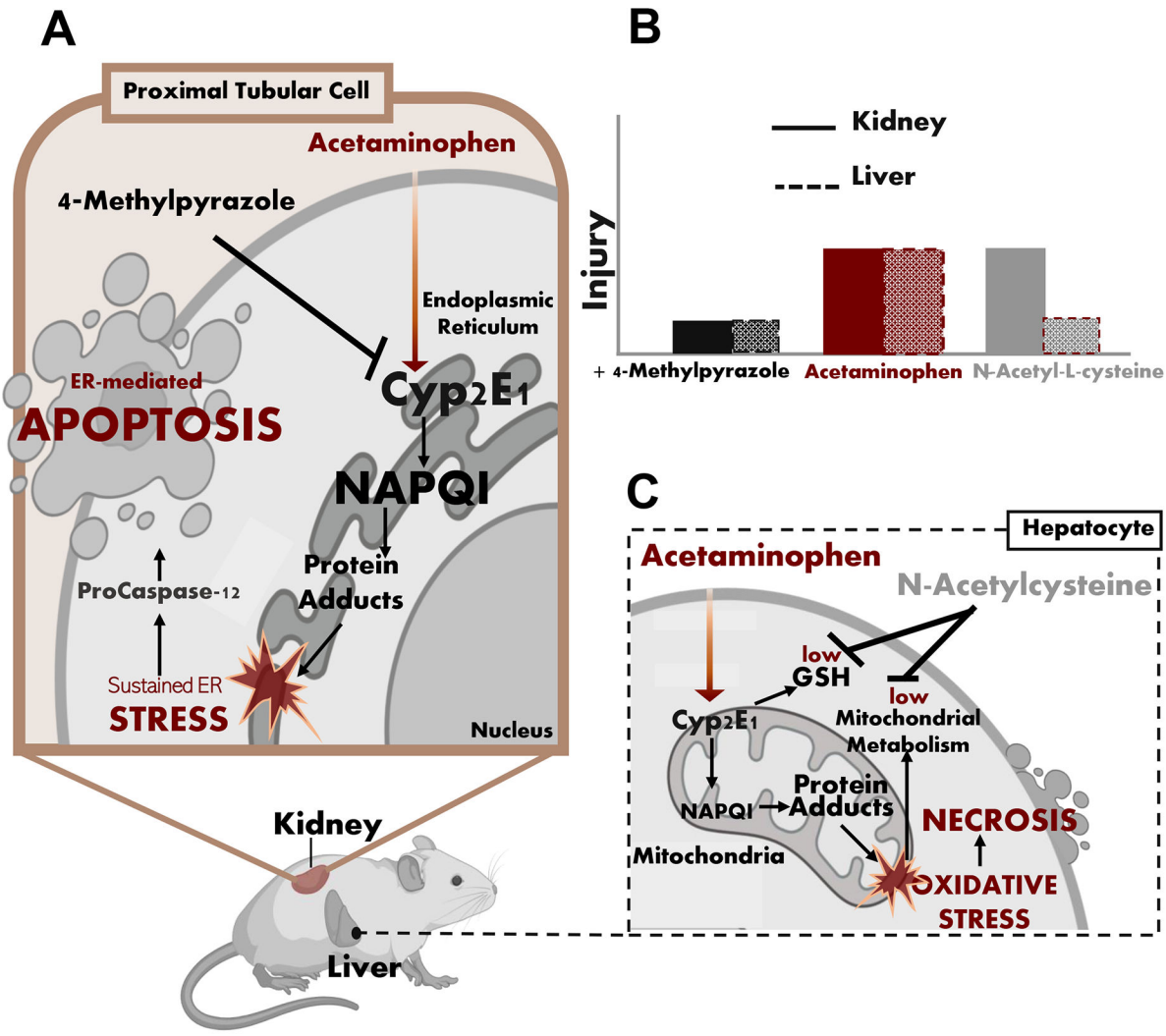

Figure 11: Mechanisms of APAP-induced hepatic necrosis and renal apoptosis.

(A) Schematic illustrations of mitochondria-induced cell necrosis in the liver after APAP overdose (B) ER stress-induced cell apoptosis in the kidney illustrations after APAP overdose and (C) inhibition of APAP-induced acute kidney injury by 4MP but not NAC.